

Mooring Line Damping In Very Large Water Depths

by
Ricardo Balzola

Master of Engineering in Logistics
*Department of Civil and Environmental Engineering
Massachusetts Institute of Technology (1999)*

Ocean Engineer and Naval Architect
Universidad Politecnica de Madrid, Spain (1997)

SUBMITTED TO THE DEPARTMENT OF OCEAN ENGINEERING
IN PARTIAL FULFILLMENT OF THE REQUIREMENTS FOR THE DEGREE OF
MASTER OF SCIENCE IN NAVAL ARCHITECTURE AND OCEAN
ENGINEERING
at the

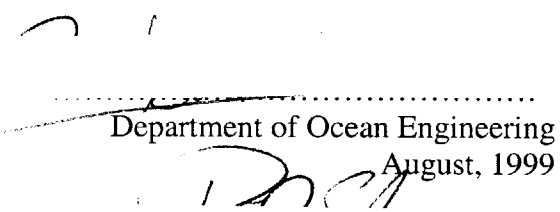
MASSACHUSETTS INSTITUTE OF TECHNOLOGY

September 1999

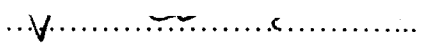
© 1999 Ricardo Balzola, All Rights Reserved

The author hereby grants to MIT permission to reproduce and distribute publicly paper
and electronic copies of this thesis document in whole or in part

Signature of the Author.....

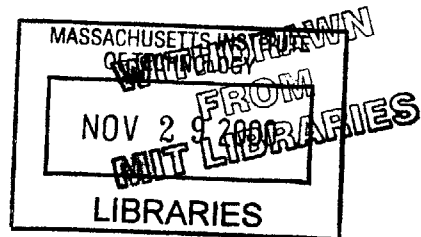

Department of Ocean Engineering
August, 1999

Certified by


Paul D. Slavounos
Professor of Naval Architecture
Thesis Supervisor

Accepted by.....


Professor A. Baggeroer
Chairman, Departmental Committee on Graduate Studies



Mooring Line Damping In Very Large Water Depth

by

Ricardo Balzola

Submitted to the Department of Ocean Engineering
on August , 1999, in partial fulfillment of the
requirements for the degree of
Master of Science in Naval Architecture and Ocean Engineering

Abstract

Precise position and motion control are indispensable factors for the operation of offshore platforms. Mooring systems are, by all means, the most common devices to obtain the required control.

The response to the motions of the platform performed by the moor will, in many cases, dictate the overall offshore platform behavior as a result of environmental loads. These loads induce in the system two typical modes of oscillation; slow drift and wave frequency motions.

The objective of this thesis is to investigate the dynamic responses and the damping achieved by cable and synthetic mooring systems when the water depth is very large. Numerical simulations for different modes of oscillation and initial conditions of the mooring lines have been executed, as to establish a comparison between the dynamic properties of the diverse mooring solutions.

Finally, in order to analyze the relative importance of the mooring damping results, the platform-moor systems are approximated to a one-dimensional mechanical damped oscillator. This approximation highlights the motion modes where the moor response is critical as well as exploring the advantages and disadvantages of each mooring solution.

Thesis supervisor: Professor Paul D. Sclavounos

Title: Professor of Naval Architecture

Acknowledgements

First of all, I would like to thank my parents for all the support and help they have given me throughout my life.

I wish to thank Jennifer, her patience with me is enormous, her help and encouragement when I most needed has been crucial for me to be able to finish this work in time. Thank you very much Jennifer, you really deserve it.

I also want to thank my advisor, Professor Paul Sclavounos, for his guidance during this last 18 months. I want to thank him how much I have learnt from him, not only about science and physics, but also about life and motivation. It has been very hard but also very educating.

I also want to thank Sungeun Kim, who has made possible this thesis helping me understand LINES 1.1 and obtain the results that are the basis for this work.

Finally, I want to thank the rest of my family, and friends, those over here and those in Spain, for making my life so enjoyable and fulfilling.

CHAPTER 1: INTRODUCTION **9**

1.1	MOTIVATION	9
1.2	OFFSHORE PLATFORMS	10
1.3	MOORING SYSTEMS	11
1.4	THESIS OVERVIEW	11

CHAPTER 2: MATHEMATICAL FORMULATION: **13**

2.1.	PLATFORM DYNAMICS FORMULATION:	13
2.2.	MOORING LINE FORMULATION:	14
2.2.1.	CHARACTERISTIC EQUATIONS OF THE LINES	14
2.2.2.	INTERNAL FORCES:	17
2.2.3.	EXTERNAL FORCES:	18
2.2.4.	BOUNDARY CONDITIONS:	23
2.3.5.	INTERACTION WITH THE SEABED:	24
2.4.	MOORING LINE DAMPING GENERATION	25
2.4.	WHOLE MOORING SYSTEM FORMULATION	28

CHAPTER 3: INITIAL CONFIGURATIONS **29**

3.1.	MAIN CHARACTERISTICS OF THE SPAR PLATFORM:	31
3.2.	MAIN CHARACTERISTICS OF THE MOORING SYSTEMS:	32
3.2.1.	CABLE MOORING SYSTEM SOLUTION	33
3.2.2.	SYNTHETIC MOORING CONFIGURATIONS:	35

CHAPTER 4: NUMERICAL RESULTS. **40**

4.1.	COMPARISON OF THE DYNAMIC PROPERTIES OF THE FOUR MOORS	40
4.2.	SLOW DRIFT OSCILLATION:	41

4.3.LINEAR SURGE OSCILLATIONS	49
4.4.HEAVE OSCILLATIONS	55
<u>CHAPER 5: DAMPING RELATIVE IMPORTANCE</u>	<u>60</u>
5.1 LINEAR DAMPED OSCILLATOR	60
5.2. PLATFORM-MOOR COEFFICIENTS	63
5.3 LINEAR APPROXIMATION	65
<u>CHAPTER 6: CONCLUSIONS</u>	<u>72</u>
<u>REFERENCES:</u>	<u>74</u>
<u>APPENDIX A: ROPE PROPERTIES</u>	<u>76</u>

Index of Tables:

Table 2-2: Viscous coefficients.....	21
Table 3-1: Main Characteristics of Spar Hull.....	31
Table 3-2: Main Characteristics of cable mooring system.	33
Table 3-3: Synthetic moor line’s properties	38
Table 4-1: Equivalent excursion for slow-drift motions	41
Table 4-2: Linear surge amplitudes.....	50
Table 5-1: Linear approximation coefficients for slow drift motion.	65
Table 5-2: Linear approximation coefficients for linear surge motion.	66
Table 5-3: Linear approximation coefficients for linear heave motion.....	66
Table 5-4: Linear approximation non-dimensional coefficients for slow drift motion.....	67
Table 5-5: Linear approximation non-dimensional coefficients for linear surge motion.	67
Table 5-6: Linear approximation non-dimensional coefficients for heave motion.	68

Index of Figures:

Figure 4-18: Heave damping. Synth. Medium tension.	8
Figure 4-19: Heave damping. Synth. High tension.....	8
Figure 5-2.A: Unstable oscillation	8
Figure 5-2.B: Neutrally stable.....	8
Figure 2-1: Mooring line local coordinates	15
Figure 2-2: Mooring line segment	16
Figure 2-3: Internal tensions	18
Figure 2-4: Relative velocities	20
Figure 2-5: Static position of mooring line.....	25
Figure 2-6: Fairlead oscillations	26
Figure 2-6 A: Force of fairlead	27
Figure 2-6 C: Hysteresis Cycle	27
Figure 2-6 B: Fairlead oscillations.....	27
Figure 3-1: Spar Platform.....	30
Figure 3-2: Spar platform dimensions.....	32
Figure 3-3 Catenary type mooring system.....	34
Figure 3-4: Synthetic Line pretension.....	35
Figure 3-5: Moor static restoring forces.....	36
Figure 3-6: Synthetic mooring system	39
Figure 4-1: Slow drift damping. Cable.....	42
Figure 4-2: Slow drift damping. Synth. Low tension.....	42
Figure 4-3: Slow drift damping. Synth. Medium tension.....	43
Figure 4-4: Slow drift damping. Synth. High tension.....	43
Figure 4-5: Slow drift damping. Period 50 s.	45
Figure 4-6: Slow drift damping. Period 100 s.	45
Figure 4-8: Slow drift hysteresis Cycles. Period 100s.	47
Figure 4-9: Linear surge damping. Cable.....	51
Figure 4-10: Linear surge damping. Synth. Low tension.....	51
Figure 4-11: Linear surge damping. Synth. Med. tension.....	52

Figure 4-12: Linear surge damping. Synth. High tension..... 52

Figure 4-13: Linear surge damping. Period 10 s.....53

Figure 4-14: Linear surge hysteresis cycles. Period 7s. 54

Figure 4-15: Linear surge hysteresis cycles. Period 15s. 55

Figure 4-16: Heave damping. Cable.....56

Figure 4-17: Heave damping. Synth. Low tension.....56

Figure 4-18: Heave damping. Synth. Medium tension.....57

Figure 4-19: Heave damping. Synth. High tension..... 57

Figure 4-20: Vertical damping. Period 10s. 58

Figure 4-21: Heave hysteresis Cycles. Period 10s.....59

Figure 5-1: Simple model for damped oscillator. 60

Figure 5-2.A: Unstable oscillation..... 62

Figure 5-2.C: Damped oscillations..... 62

Figure 5-2.B: Neutrally stable..... 62

Figure 5-2.D: Collapse response62

Figure 5-3: Natural oscillation for slow drift linear approximation..... 69

CHAPTER 1:

INTRODUCTION

1.1 Motivation

Precise position and motion control are indispensable factors for the operation of offshore platforms. Although there are other means of obtaining this control, mooring lines are, without any doubt, the most important solution.

Among the mooring line solutions, there are at least two subdivisions. One division is the vertical tension leg mooring, for which the buoyancy of the platform exceeds the weight, and the cables provide the net equilibrating force.

The second class, which is the object of study of this thesis, are the spread mooring systems, that consist of several pre-tensioned anchor lines arrayed around the structure to hold the mooring in the desired position. This thesis will study in detail the dynamics of this type of mooring systems for large water depths.

1.2 Offshore Platforms

Offshore platform designs vary from gravity platforms sitting on the seabed, to semi-submergible platforms, purely large free-floating bodies. The semi-submergible offshore platforms are used for large to very large water depths, and are typically kept in position by a spread mooring system. A set of pipes and risers are used to connect this floating structure with the exploration and drilling equipment on the seabed.

Semi-submergible platforms are subject to environmental loads, mainly created by waves, wind and ocean currents. These environmental loads induce motion responses on the platform-moor group. Typically, motions of floating structures can be divided into wave-frequency, high frequency, and slow drift motions.

The wave frequency motion is mainly produced by first order interactions between waves and the floating body. The amplitude and frequency of these motions are, in general, similar to those of the waves that induce them.

High frequency motions are generated by non-linear wave excitation. Their natural periods are in the order of two to four seconds and they are frequently significant for TLP structures. They are out of the scope of this thesis, since they do not appear in catenary-type moored platforms.

Similar non-linear interactions between the floating body and the waves cause slow and mean drift motions. This kind of motion appears in every type of floating platform. They arise from resonant slow-drift oscillations. The typical period of these oscillations are in the range of 50 to 150 seconds for conventional moored platforms. This type of motion for a moored floating body typically occurs in surge, sway and yaw. Slow drift motions are characterized by large horizontal excursions of the platforms that drive, as a result, enormous forces on the mooring lines.

These types of oscillations are critical in catenary type moored platforms and are being studied in this thesis.

1.3 Mooring systems

Spread mooring systems hold semi-submersible platforms and floating production ships in their desired position. Moreover, the moor provides the floating body the required restoring forces to return to that equilibrium position when environmental loads force the structure away from it.

The increasing water depth of oil exploration and drilling is creating the necessity for new solutions of spread mooring systems. Cable moors are becoming increasingly expensive for very large water depths, since the complexity of their installation is growing rapidly due to the large weight of the lines. Therefore, lighter moorings are becoming more attractive, especially for large water depths.

This thesis studies and compares three synthetic mooring solutions with a regular cable-catenary type moor. The static and dynamic responses of these moors has been studied in order to compare the restoring and damping properties among each of these four solutions.

1.4 Thesis overview

This thesis has been divided into six chapters.

Chapter two covers the analytical formulation of the problem, starting with a brief review of platform dynamics, and then deriving the characteristic equations of the mooring lines. This mooring line formulation neglects the contribution of bending effects. Finally this

chapter covers the derivation of energy absorption achieved by the lines and moor as they are forced to undergo oscillatory motions.

Chapter three presents the platform specifications that have been used as a base for this study and the mooring line designs that have been tested along this thesis. These designs include material and geometrical properties as well as all the static responses of the different systems to offset the fairlead from the initial position.

Chapter four presents the numerical results of the motion simulations for the mooring line designs. These results present the dynamic properties of the mooring systems for 3 distinct modes of oscillation, slow drift surge, wave frequency surge and finally wave frequency heave motions. Diverse amplitudes and periods have been used for all mooring systems in order to understand the non-linear dynamics of these simulations.

Chapter five compares the results from chapter four using a linear damped oscillator. A brief introduction to the formulation of a linear damped oscillator is included in this section. Then, the mooring damping results from chapter four and the restoring forces of chapter three are converted to the constant coefficients that the formulation of the damping physical approximation requires. The results from this approximation are displayed in this chapter.

The computations presented in this thesis were carried out with the computer program LINES 1.1 licensed by Boston Marine Consulting Inc. Further details on the methods presented in this thesis along with the capabilities of LINES 1.1 may be found in the LINES 1.1 user manual which can be downloaded from the BMC web site at www.bmarc.com.

Finally chapter six draws the main conclusions of the thesis.

CHAPTER 2:

MATHEMATICAL FORMULATION:

2.1. Platform Dynamics formulation:

The dynamics of a floating offshore structure can be modeled through a second order coupled linear system of differential equations. For all practical purposes, the platform is considered a rigid structure with 6 degrees of freedom. The general equation for such a system can be expressed in matrix form as:

$$[M + A] \frac{d^2 \vec{x}}{dt^2} + [B] \frac{d\vec{x}}{dt} + [C] \vec{x} = \vec{F}(t) \quad (2.1)$$

Where the \vec{x} is a 6x1 vector that holds the six degrees of freedom that characterize the response of the structure. The first three values of this vector represent the platform translations along the coordinate system axes while the last three values describe rotations around these same axes. M, A, B and C are six by six matrices that incorporate the mass, added mass, damping and restoring coefficients of the floating structure. The

magnitude and distribution of the coefficients in these matrices reflect the dynamic and static characteristics of each degree of freedom and the coupling effects among them.

The force term in the previous equation comprises the sum of all the environmental loads to the floating body plus the force due to the mooring system. For all practical purposes, the forces on the fairlead of the mooring lines are, as those of the platform, dependent on acceleration, velocity and position of the system. Therefore, it is natural to bring them to the left-hand side of the equation.

Not all the contributions, however, of the moor to the L.H.S. matrices are equally important. The inertia related terms for the mooring system are very small compared to those of the platform. The mass and added mass of the mooring lines are several orders of magnitude smaller than those of the platform.

On the other hand, the contribution to the damping and restoring coefficients are very important, and in some cases they are the dominant contribution to the damping and restoring forces. For example, the restoring coefficient in sway, surge or yaw comes solely from the mooring system. To fully understand the dynamics of a floating platform, we must comprehend the interaction between this body and the mooring that maintains at a fixed position.

2.2.Mooring Line Formulation:

2.2.1.Characteristic equations of the lines

Let a generic mooring line be defined by the so-called natural coordinates of a 3-dimensional line. The anchor end in the material line would be defined as the origin and the direction towards the fairlead as positive along the cable.

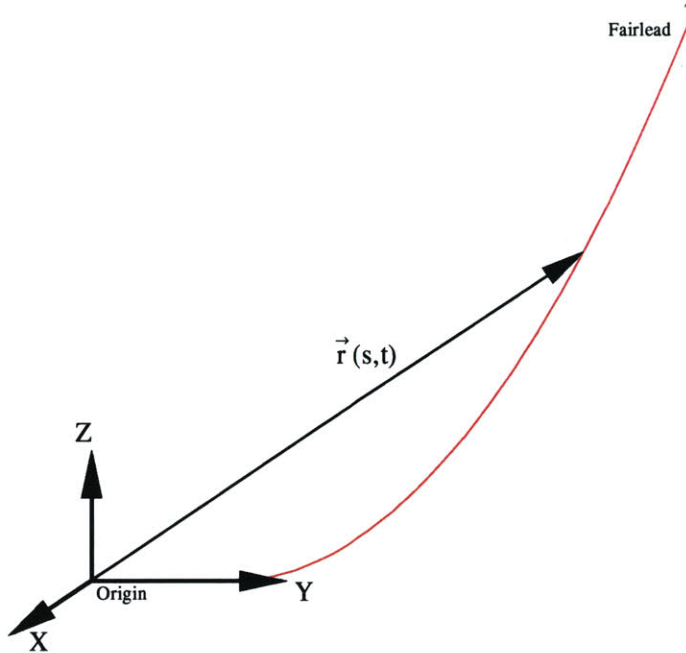


Figure 2-1: Mooring line local coordinates

Let “s” be the Lagrangian distance from a given point of the mooring line to the origin when the line is not stretched. The coordinates of any material point of the mooring line can be expressed as a function of its position along the cable and the time as follows,

$$\vec{r}(s, t) = (x(s, t), y(s, t), z(s, t)) \quad (2.2)$$

Once a tension is applied, and provided that the mooring line is made of elastic material, the cable would stretch. Let “s₁” be the stretched distance measured from a given material point to the origin of the line. In general this distance is a function of the original s and the time so it can be expressed as s₁(s,t).

Given the previous definitions for the unstretched and stretched distance along the line, s and s₁, the next step will be to introduce the concept of strain or rate of strain(ε) in the line.

Strain ϵ : A cable segment with unstretched length s has at some point a Lagrangian arclength of s_1 . Let the strain ϵ then be defined as follows:

$$\epsilon = \lim_{\delta s \rightarrow 0} \left(\frac{\delta s_1 - \delta s}{\delta s} \right) = \frac{ds_1}{ds} - 1 \Rightarrow \frac{ds_1}{ds} = 1 + \epsilon \quad (2.3)$$

Let then \vec{t} be the tangential vector to the stretched position of the material line. As such it can be expressed as the first derivative of the vector \vec{r} with respect to s_1 , the stretched distance. Then,

$$\vec{t} = \frac{d\vec{r}}{ds_1} = \frac{d\vec{r}}{ds} \cdot \frac{ds}{ds_1} = \frac{d\vec{r}}{ds} \frac{1}{1 + \epsilon} \Rightarrow \frac{d\vec{r}}{ds} = (1 + \epsilon) \vec{t} \quad (2.4)$$

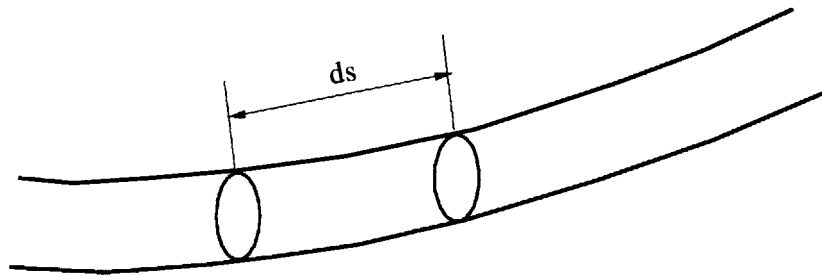


Figure 2-2: Mooring line segment

If we focus now on a differential segment of mooring line of length ds , we see that any of such differential segments of its line is governed by two fundamental equations. The first one is a constitutive relation similar to the continuity principle for fluid dynamics. For any given part of the mooring line it is known that,

$$\vec{t} \cdot \vec{t} = 1 \quad (2.5)$$

Since the tangential vector is always a unit vector, this is always true.

Then combining equation 2.4 and equation 2.5 we obtain,

$$\frac{d\vec{r}}{ds} \frac{d\vec{r}}{ds} = (1 + \epsilon)^2 \cong 1 + 2\epsilon \quad (2.6)$$

The second equation that governs the mooring line motion is Newton's Law that can be expressed as,

$$m \frac{d^2 \vec{r}}{dt^2} = \sum \text{External Forces} + \sum \text{Internal Forces} \quad (2.7)$$

2.2.2. Internal Forces:

The fundamental internal force present in a mooring line is the tension. For mooring lines, it is a normal practice to introduce the concept of an effective tension T_e . This tension is defined by:

$$T_e = T + P_f A_f \quad (2.8)$$

Where,

P_f is the fluid pressure in the position of this particular segment of the mooring line discarding the line-induced disturbance and, A_f is the cross sectional area of the line.

The utilization of the effective tension causes the mooring line equations to look like their equivalent in air with the exception that when calculating the force due to the weight of the cable or line, the regular weight must be replaced by the weight of the line in water.

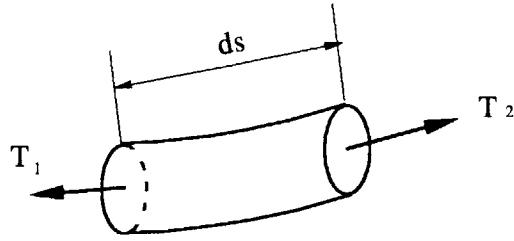


Figure 2-3: Internal tensions

The tension inside the line will, generally, have the same direction as the line itself. Therefore, the internal force on a segment with unstretched length can be written as:

$$\text{Internal Force} = \frac{d}{ds} (T_e \vec{t}) ds = \frac{d}{ds} \left(\frac{1}{(1+\epsilon)} T_e \frac{d\vec{r}}{ds} \right) ds \quad (2.9)$$

2.2.3. External Forces:

The external forces to a segment of mooring line can be subdivided into 3 components,

F_1 due to weight and buoyancy effects

F_2 due to flow inertial effects. (Added mass related forces)

F_3 due to fluid viscous effects.

Line Weight. Buoyancy.

The total vertical force of the segment due to weight and buoyancy effects is given by:

$$\vec{F}_1 = (g\rho_f A_f - w) ds \cdot \vec{k} \quad (2.10)$$

Where,

ρ_f is the fluid density and,

w is the line weight in water per unit length.

Added mass forces:

The inertia related forces can be divided into two different components. The first one is due to the motion of the fluid around the mooring line segment. The second component is to the motion of the segment itself considering the fluid surrounding it stationary.

For the calculation of both of these terms we will need the following linear operator, [N], which is a 3x3 matrix, that multiplied by a vector, yields the component of this vector normal to the mooring line. Lets define [N] as,

$$[N] = [I] - \left[\frac{d\vec{r}}{ds} \right]^T \left[\frac{d\vec{r}}{ds} \right] \quad (2.11)$$

With the aid of the matrix [N] and using GI Taylor's Theorem to calculate the normal inertial forces, the added mass terms exerted upon the line are split into,

$$\vec{F}_{21} = \rho_f A_f ds (1 + C_m) [N] \frac{d\vec{v}_f}{dt} \quad (2.12)$$

Due to the fluid velocity \vec{v}_f around a fixed segment and,

$$\vec{F}_{22} = -\rho_f A_f ds (C_m) [N] \frac{d^2\vec{r}}{dt^2} \quad (2.13)$$

Due to the acceleration of the material segment $\frac{d^2\vec{r}}{dt^2}$ assuming the surrounding fluid is stationary.

Note that the flow velocity and acceleration are free of disturbance effects caused by their interaction with the line. This last fact being only an approximation is very reasonable, since the flow is most affected by other large structures as the platform itself or the flow initial velocity components due to currents or waves. Taking into account the possible disturbances in the flow due to the presence of the mooring line would make the problem far more complicated and provide only marginal changes to the final result.

Viscous Fluid Forces.

The viscous term of the force is going to be calculated using Morison’s equation for both the normal and tangential directions of the segment. For this calculation to be possible we need the relative velocity between the segment and the fluid that surrounds it.

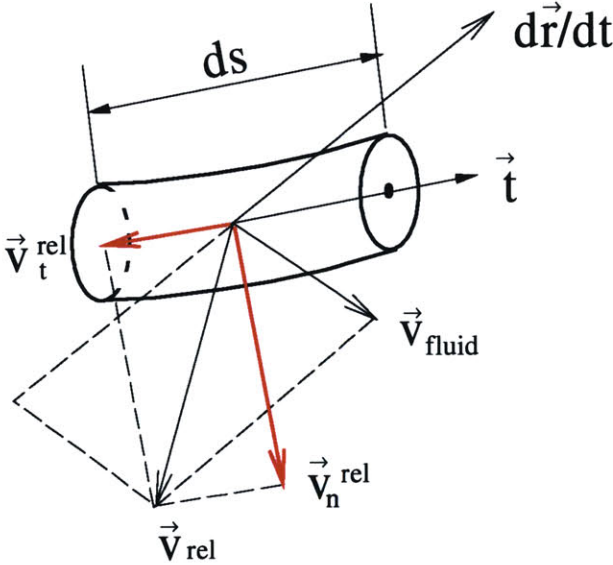


Figure 2-4: Relative velocities

The relative velocity between the line segment and the fluid is defined by

$$\vec{v}^{rel} = \vec{v}_f - \frac{d\vec{r}}{dt} \tag{2.14}$$

Now, if we decompose this relative velocity in tangential and normal direction relative to the mooring line we obtain,

$$\vec{v}_n^{rel} = [N]\vec{v}^{rel} \quad (2.15)$$

for the relative normal velocity and,

$$\begin{aligned} \vec{v}_t^{rel} &= (\vec{t} \cdot \vec{v}^{rel})\vec{t} = \left(\frac{1}{1+\varepsilon} \frac{d\vec{r}}{ds} \cdot \vec{v}^{rel} \right) \frac{1}{1+\varepsilon} \frac{d\vec{r}}{ds} = \frac{1}{(1+\varepsilon)^2} \left(\frac{d\vec{r}}{ds} \cdot \vec{v}^{rel} \right) \frac{d\vec{r}}{ds} \Rightarrow \\ \vec{v}_t^{rel} &\cong \frac{1}{1+2\varepsilon} \left(\frac{d\vec{r}}{ds} \cdot \vec{v}^{rel} \right) \frac{d\vec{r}}{ds} \end{aligned} \quad (2.16)$$

for the relative tangential velocity. Once we know this two components of the relative velocity the viscous force acting along the line can be approximated through Morrison's equation in both directions as,

$$\vec{F}_3 = \frac{1}{2} \rho_f \left(D_n C_d |\vec{v}_n^{rel}| \vec{v}_n^{rel} + \pi D_t C_f |\vec{v}_t^{rel}| \vec{v}_t^{rel} \right) ds \quad (2.17)$$

Where D_n is the projected dimension normal to the line and πD_t is nothing but the length of a circle of diameter D_t . These two dimensions are a function of the mooring line geometry and in the case of a regular cable mooring line, they are the same and coincident with the maximum diameter of the cable. C_d and C_f are, respectively, the drag and friction coefficients. As well as the previous two diameters, these two coefficients depend mainly on the mooring line geometry. See the next table as an example of the range of these coefficients.

Mooring line type	C_d	C_f
Cable-type	O(1)	O(0.01)
Chain-type	O(1)	O(0.1)

Table 2-2: Viscous coefficients

Now, substituting all the forces from formulas (2.9), (2.10), (2.12), (2.13) and (2.17) into Newton's law (2.7) and substituting the initial mass in the original equation by a linear density times the length of the segment yields

$$m(s)ds \frac{d^2 \vec{r}}{dt^2} = \begin{cases} \frac{d}{ds} \left((1 + \varepsilon)^{-1} T_e \frac{d\vec{r}}{ds} \right) ds \\ (g\rho_f A_f - w) ds \cdot \vec{k} \\ \rho_f A_f ds (1 + C_m) [N] \frac{d\vec{v}_f}{dt} \\ - \rho_f A_f ds (C_m) [N] \frac{d^2 \vec{r}}{dt^2} \\ \frac{1}{2} \rho_f (D_n C_d |\vec{v}_n^{rel}| \vec{v}_n^{rel} + \pi D_t C_f |\vec{v}_t^{rel}| \vec{v}_t^{rel}) ds \end{cases} \quad (2.18)$$

Eliminating the differential of length ds from all the terms and reallocating the first and forth terms in the right hand side yields to the definitive momentum equation

$$[M] \frac{d^2 \vec{r}}{dt^2} - \frac{d}{ds} \left(\frac{1}{(1 - \varepsilon)} T_e \frac{d\vec{r}}{ds} \right) = \begin{cases} (g\rho_f A_f - w) \vec{k} \\ \rho_f A_f (1 + C_m) [N] \frac{d\vec{v}_f}{dt} \\ \frac{1}{2} \rho_f (D_n C_d |\vec{v}_n^{rel}| \vec{v}_n^{rel} + \pi D_t C_f |\vec{v}_t^{rel}| \vec{v}_t^{rel}) \end{cases} \quad (2.19)$$

Where $[M]$ is the mass matrix defined as follows

$$[M] = m(s)[I] + \rho_f A_f C_m [N] \quad (2.20)$$

Now, by using Hooke's Law and assuming that the volume per unit length of the cable will remain unchanged with strain, it is implied that Poisson's ratio μ is equal to 0.5, the line strain ε can be rewritten as

$$\varepsilon = \frac{T_e}{EA_s} \quad (2.21)$$

And plugging this definition of the line strain into the original “Continuity” equation (2.6) leads to the following constitutive relation:

$$\frac{d\vec{r}}{ds} \frac{d\vec{r}}{ds} = 1 + 2 \frac{T_e}{A_s E} \quad (2.22)$$

that can be rewritten as:

$$T_e = \frac{A_s E}{2} \left(\frac{d\vec{r}}{ds} \frac{d\vec{r}}{ds} - 1 \right) \quad (2.23)$$

Momentum equation (2.19) plus this last constitutive relation (2.23) comprise a full close form of equations to study the dynamics of a mooring line. From this system we are able to obtain the displacement of every segment, $\vec{r} = (s, t)$, and the effective tension, T_e .

However, for the problem to be complete, these equations have to be supplemented with two extra requirements. On one hand, the non-linear system of partial differential equations requires a set of boundary conditions, and on the other hand, due to the nature of the problem, the interaction of the mooring line with the seabed requires a special treatment.

2.2.4. Boundary Conditions:

Although different authors [9] use different boundary conditions, probably the most natural set of conditions for catenary-like problems are the positions of both ends of the mooring line. Therefore LINES 1.1 uses the following as boundary condition inputs. The first boundary condition is given by fixing the position of the anchor to the line coordinate system origin. The second B.C. is simply given by the position of the fairlead

in time referred, again, to the same mooring line coordinate system. These two conditions can be expressed as follows,

$$\vec{r}(0,t) = \vec{0} \quad (2.24)$$

$$\vec{r}(L,t) = \vec{R}(t) \quad (2.25)$$

Where $s=0$ is nothing but the origin in arclength of the mooring line and L is the maximum unstretched arclength of the line and consequently where the fairlead stands.

2.3.5. Interaction with the seabed:

Typical wire rope and chains used in mooring systems have generally a significant length of line that lies on the ocean floor. The interaction with the seabed adds a new dimension to the classic catenary problem. Apart from the exterior forces that have been discussed up to now, introducing the presence of the seabed adds another force to the problem. Any part of the mooring line laying on the plane $z=0$ gets a supporting force from the seabed that cancels out the remaining weight of that particular part of the line.

To solve this problem, LINES uses the following approach: Whenever any segment of the mooring line lays under the $z=0$ plane, the regular weight force of the segment is inverted to point upwards. The idea is to create an artificial medium below the seabed with a higher density than the mooring line. The density in this artificial medium is linear; it has a value equal to the density of the mooring line for $z=0$ and increases linearly as z tends to higher numbers in the negative range. With such a medium the segments of the mooring line that might be under the seabed will eventually float to the surface of the seabed as the simulation runs to their real static position.

The weight and buoyancy force components that were displayed in equation (x) for $z>0$ are changed into

$$\vec{F}_1 = (gA_f \rho_s (1 - k_1 z) - w) \vec{k} \quad \text{for } z \leq 0 \quad (2.26)$$

Where k_1 is the slope of the density in the artificial medium and ρ_s is the modified density of the line. ρ_s is such that for $z=0$ the vertical force turns out to be zero as well. For any $z < 0$ the magnitude of this force would increase linearly as shown by equation 2.26.

The result of this approach is reflected in the next figure. For a given a fixed set of positions for both ends of the mooring line, O and F, the close form solution of a regular catenary line of the same characteristics can be obtained (red color in figure 2-5). When these initial conditions are run under LINES, the real shape of the mooring line, including the presence of the seabed, is obtained as the line converges to the final static position (blue line in figure 2-5).

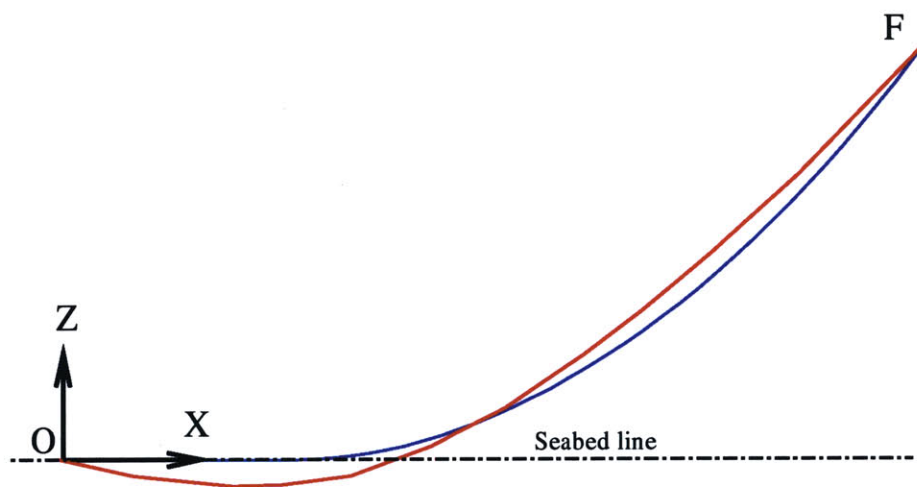


Figure 2-5: Static position of mooring line

2.4. Mooring Line Damping Generation

In order to calculate mooring induced damping, or the damping that a mooring line would introduce into a floating platform or body, the fairlead of that particular line will be forced to move under oscillatory motions either horizontally or vertically. Mooring induced damping arises due to the flow separation around the lines. This effect is

simulated in a non-linear manner by the usage of the viscous effects under Morrison's equation.

The damping contribution of the mooring line is calculated as the energy that the material line absorbs along a complete oscillation cycle. To calculate this damping, we need the pair (Tension, Position) on the fairlead for every time step along this cycle. With that pair, the damping contribution would be calculated as,

$$E = \int_t^{t+T} \vec{F}(t) \cdot \frac{d\vec{r}(L,t)}{dt} dt \equiv \oint_{\text{Period}} \vec{F}(\vec{r}) \cdot \Delta\vec{r} \quad (2.27)$$

For a further clarification of this concept, consider a mooring line subject to a forced horizontal oscillatory motion in its fairlead of amplitude A=10 m. (figure 2-6). Figures 2-7 A and B show the history and patterns of the horizontal displacement and force on the fairlead with the increasing time. If, as shown in figure 2-7.C, we plot tension on the fairlead versus displacement, we obtain the so-called hysteresis cycle. The dissipated energy per complete cycle is simply the area within a close loop.

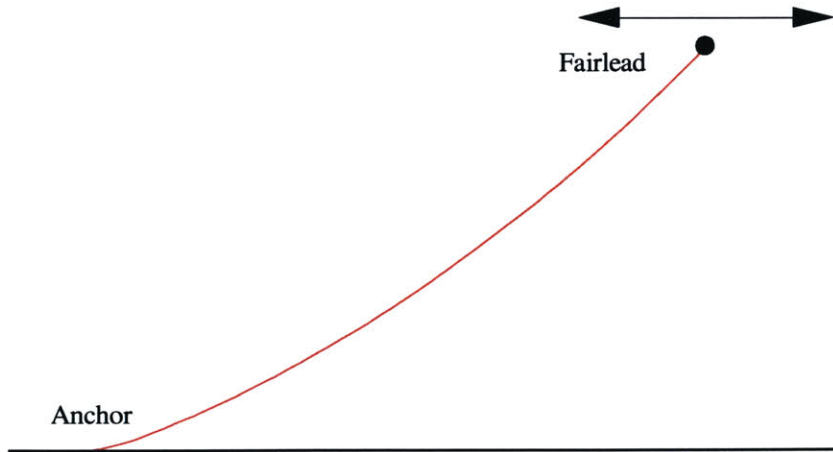


Figure 2-6: Fairlead oscillations

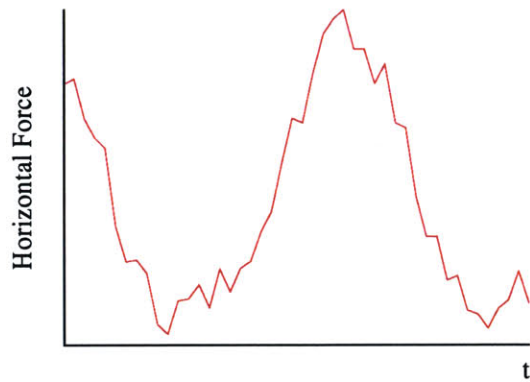


Figure 2-6 A: Force of fairlead

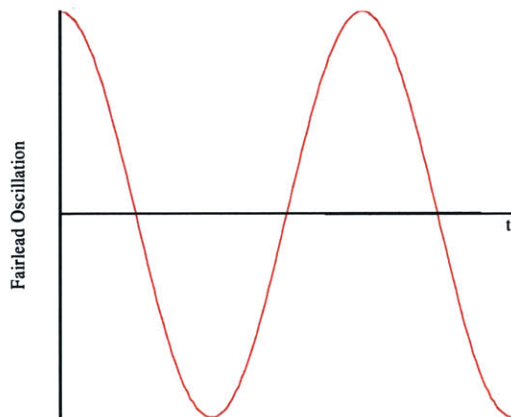


Figure 2-6 B: Fairlead oscillations

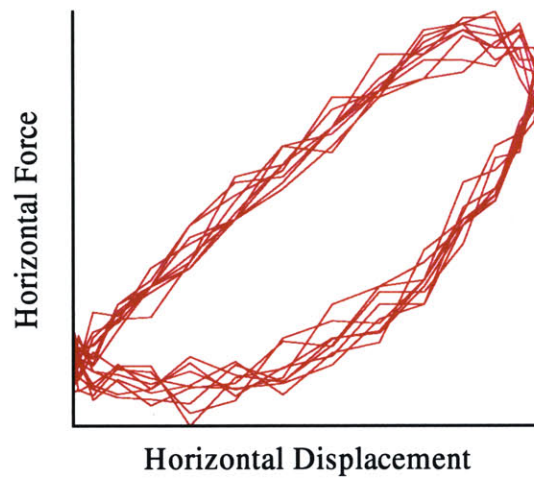


Figure 2-6 C: Hysteresis Cycle

The area embedded in the hysteresis cycle represents the amount of energy absorbed by the line in every oscillation and corresponds to the result obtained from the integration 2.27. Note that while this hysteresis loop figure presents several oscillation cycles figures A and B represent only about a period and a half of the fairlead oscillating motions and forces. It is clear from the hysteresis loop graph that the system has reached a reasonable

steady motion. Note that mooring lines, being a dynamic system, cause the results from the first period or periods in the simulation to be discharged since they are sensitive to the start-up transients.

2.4. Whole Mooring System formulation

The previous procedure for a single mooring line has been generalized to take account for the coupled responses of all the lines comprising the mooring system.

The relationships for the total force that the mooring system exerts on the platform can be found by considering the individual line contributions. In general,

$$F_i^T = \sum_{n=1}^L F_i^n \quad i = 1,2,3 \quad (2.28)$$

Where F_i^T is the total force on the direction i and L is the total number of lines. And,

$$M = \sum_{n=1}^L \vec{r}^n \times \vec{F}^n \quad (2.29)$$

Where M is the total torque that the mooring system applies into the platform and \vec{r}^n is the position of the fairlead of line n relative to the platform coordinate system.

Knowing these extensions, the damping created by the assemblage of all mooring lines creates is obtained by adding the contributions of all the forces in the integration along the complete motion loop.

CHAPTER 3

INITIAL CONFIGURATIONS

As off shore oil exploration and production moves into areas of greater ocean depths, the necessity to create and implement new concepts in mooring designs becomes increasingly apparent.

As water depths increase, the regular cable catenary moorings become less and less attractive. For large and especially very large water depths, the cable mooring lines become extremely long and heavy. This large weights and lengths carry several disadvantages. The first disadvantage is seen in the dramatic increase of the cable cost and, particularly, the cost of the moor installation. Secondly, as depth increases, the restoring force to horizontal motion decreases drastically, allowing very large horizontal excursions of the offshore system. These large offsets of the platform increase the cost of the riser solutions.

In recent years the trends of the mooring systems for offshore devices have been shifted into different approaches than the regular steel catenary moorings. Taut mooring systems using synthetic fibers are an interesting alternative. Some of the potential benefits of the usage of synthetic lines when compared with catenary mooring systems are:

- Low weight: This fact diminishes the cost of handling and installation of the mooring system.
- Smaller horizontal offsets. The offsets are reduced by a factor of 2-5 with respect to a regular catenary system.
- No potential hazard to the sub-sea equipment in case of a line breakage and fall into the seabed.
- Smaller lengths of cable that drives the total cost of the line down.

The configuration and dynamic properties of these two mooring systems, catenary-type mooring and synthetic taut mooring are, in general, different. The objective of this thesis is to perform a fully dynamic analysis of both types of mooring systems. I will also draw a comparison between the two systems and analyze the differences in performance and dynamic properties.

The base of this study is a SPAR platform already tested and in operation currently using a classical catenary-type mooring system. A Spar

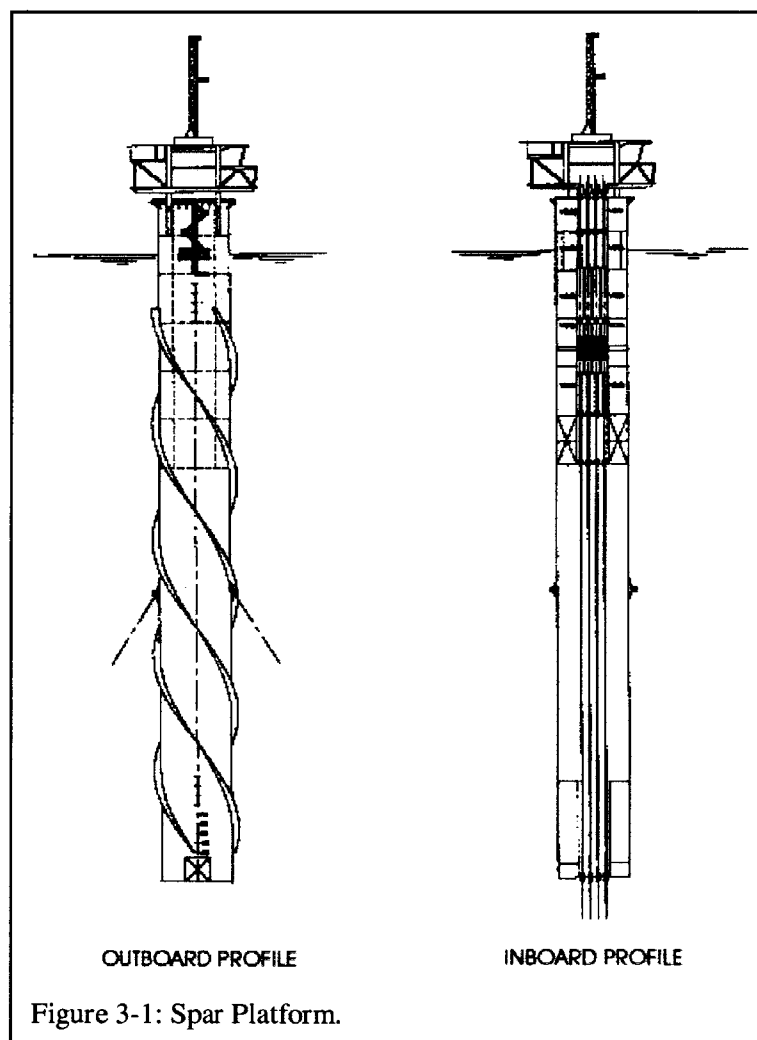


Figure 3-1: Spar Platform.

platform is a deep draft offshore structure. This type of offshore platform consists of a cylindrical hull and a deck. The hull might be used for storage purposes. The deck on this type of platform is a more typical deck that can be found on many other offshore platforms.

The analysis for all systems, the existing mooring lines and a synthetic cable taut moorings, are based on the hull motion results and the response to the environmental loads of the system. The responses of the platform to the environmental loads have been obtained from experimental data and state-of-the-art computational tools such as SWIM (Slow Wave Motion of Platforms). While only one configuration for the catenary-type has been studied since this solution has already been installed in the platform, I have run extensive experiments with different solutions for synthetic taut mooring lines.

3.1. Main characteristics of the SPAR platform:

The following table shows the main dimensions and characteristics of the hull of the Spar platform used for this thesis,

Main Characteristics of the Spar Hull	
Hull Diameter	37.18 m
Hull Length	214.85 m
Draft	198.12 m
Mass	$2.20495 \cdot 10^8$ kg

Table 3-1: Main Characteristics of Spar Hull

These previous characteristics are sketched in the next figure.

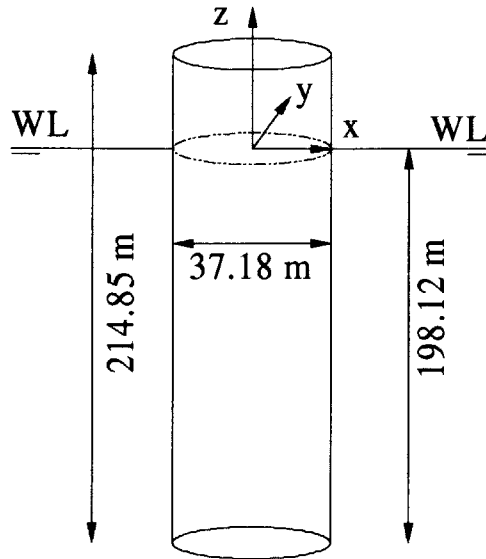


Figure 3-2: Spar platform dimensions

The weight of this type of platform and the amount of water that her hull displaces causes the platform to rest in vertical stable equilibrium. The purpose of the moor is to hold the platform over a specific point of the seabed and not to fix her vertical position. However, given the shape and position of lines in the mooring systems, the platform receives an extra vertical tension that pulls it down. The magnitude of this tension is very small compared to the buoyancy or the weight effects of the platform.

3.2. Main characteristics of the mooring systems:

The platform is held at a fixed position by the mooring system. This mooring system provides the platform with the restoring forces and damping to balance out the displacements and motions that the environmental loads induce on the floating structure. This platform particular moor consists on a set of 14 lines evenly distributed in a circular shape around the hull. The geometry and physical properties of all the lines are the same. This study consists of full numerical dynamic simulations for each different set of mooring lines. The first test coincides with the existing one in the platform, while the rest are based on synthetic lines. All these synthetic lines will have similar material properties, but different initial pretensions. To achieve the variation in the pretension of

the lines, the initial position of the anchor is going to be variable. The rest of the geometrical properties of these lines are going to be the same so that the reason for all possible differences in the dynamic properties is only due to the initial pretension.

3.2.1.Cable Mooring System Solution

The cable mooring solution is already installed and tested for this particular platform. For this reason, it will be used as a basis for the comparison of the static and dynamic properties of all the new synthetic configurations. The following table shows the configuration of the catenary-type mooring line cables,

Catenary-type mooring line configuration (For each line)	14 lines Moor
Fairlead Depth	106.68 m
Horizontal distance from Fairlead to Spar vertical axis	18.59 m
Anchor Depth	789.4 m
Horizontal distance from Anchor to Spar vertical axis	838 m
Total Line Length	1082 m
Pretension at Fairlead	2055 KN
Weight in water (per unit length)	1116.6 N/m
Weight in air (per unit length)	1350 N/m
Diameter	0.172 m
EA	$1.824 \cdot 10^9$ N
Added Mass Coefficient	1
Viscous drag Coefficient	1.2
Viscous Friction Coefficient	0.05

Table 3-2: Main Characteristics of cable mooring system.

The result of the geometric properties displayed in the previous table is shown in the next figure that shows the arrangement of the mooring line cables around the platform. Such a

symmetric disposition of the lines ensures a similar response from the moor to any horizontal motions of the complete system regardless of the direction of the excitation.

The existence of such a large number of mooring lines increases the safety qualities of the mooring system. In case of failure of any of the lines of the moor, given the large number lines present, the stresses would be spread among the rest of the lines, preventing any of them from reaching any tension above the critical breaking tension.

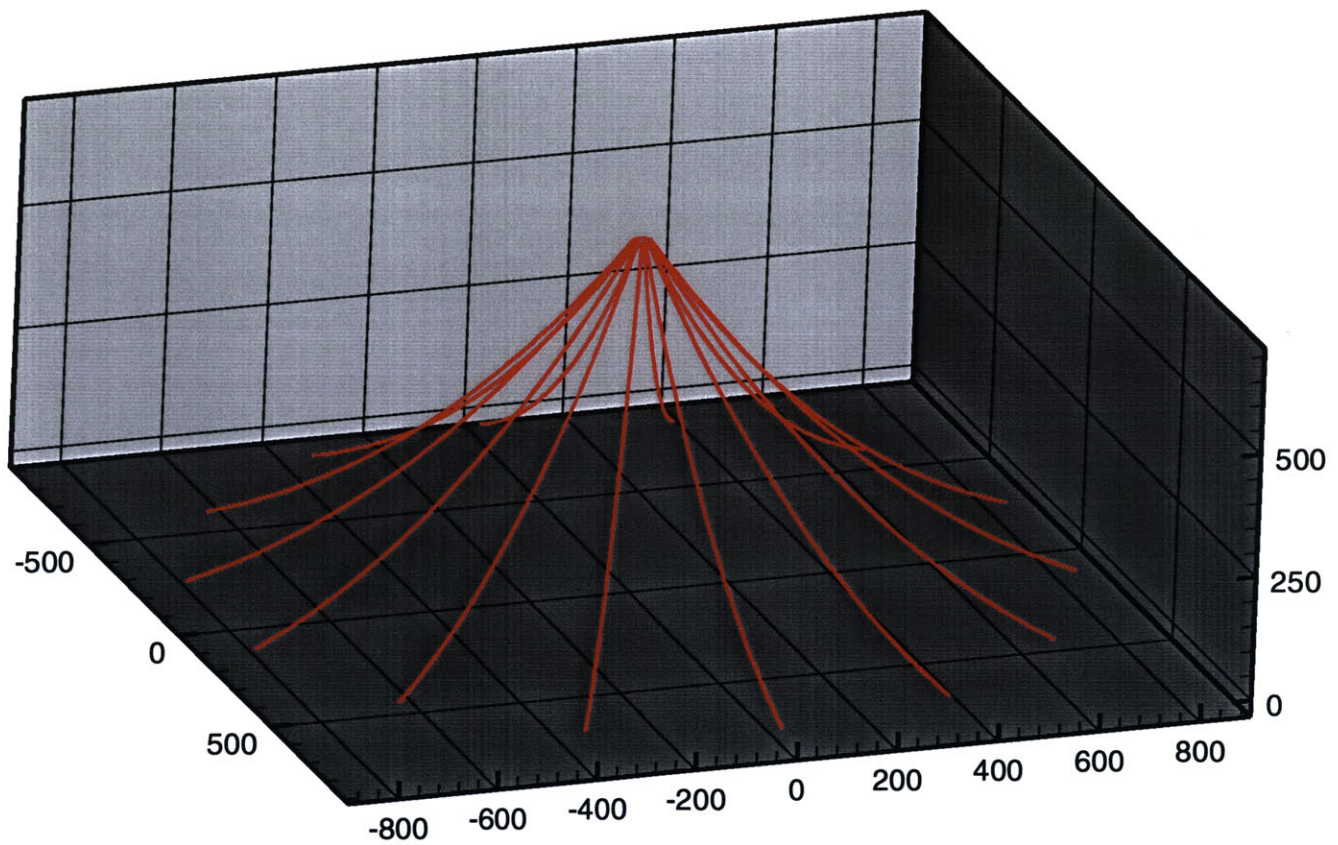


Figure 3-3 Catenary type mooring system.

3.2.2.Synthetic Mooring Configurations:

All the synthetic lines tested configurations are also composed of a set of 14 lines evenly distributed around the vertical axis of the platform. The fundamental reason behind this decision was to eliminate all possible reasons of misleading results of the experiments. A secondary reason for using the set of 14 lines is to ensure similar safety qualities and to preserve the axisymmetric properties of the moor.

To maintain the uniformity of the experiments, the material properties of the synthetic lines are the same for all three of the synthetic mooring solutions subject to study in this thesis. The difference among these three solutions is the initial pretension of the lines in each moor. In order to achieve these diverse pretensions on the lines, the distance of the anchor to the vertical axis of the platform is varied from one solution to the next. The next figure shows how the tension of the fairlead of the line varies with the distance of the anchor to the vertical position of the platform axis.

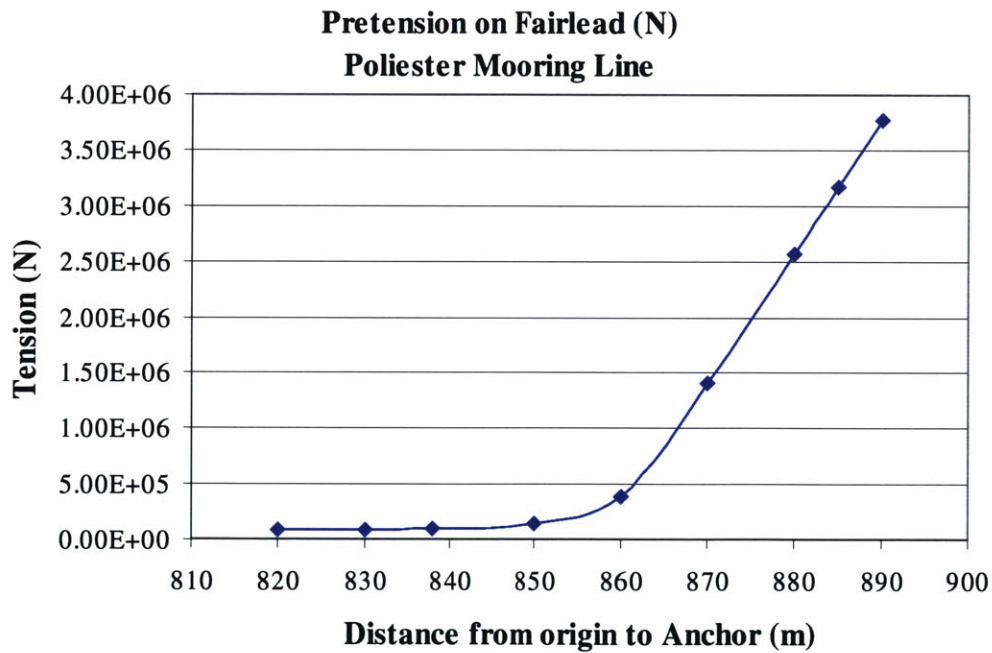


Figure 3-4: Synthetic Line pretension

Figure 3-4 presents a very large change in behavior of the pretension of the line for distances from the anchor to the vertical of the platform over 860 meters. The total unstretched length of the line is maintained constant. When the horizontal distance from the anchor to the platform is smaller than 860 meters, the lines present a loose shape, however, as soon as the distance reaches that limit the lines became taut and the pretension increases dramatically.

To decide what set of pretensions are valid to maintain the platform position, the restoring forces against horizontal excursions of the platform was studied. Any synthetic configuration that would provide smaller restoring forces than the actual cable solution was discharged automatically. A static study of the restoring forces for the whole moor was carried out for a range of anchor-to-origin distances from 820 to 870 meters. The results of this study are displayed in the next figure.

Restoring Forces for the Whole Moor. 8 Different Synthetic Configurations and the original platform Cable Moor.

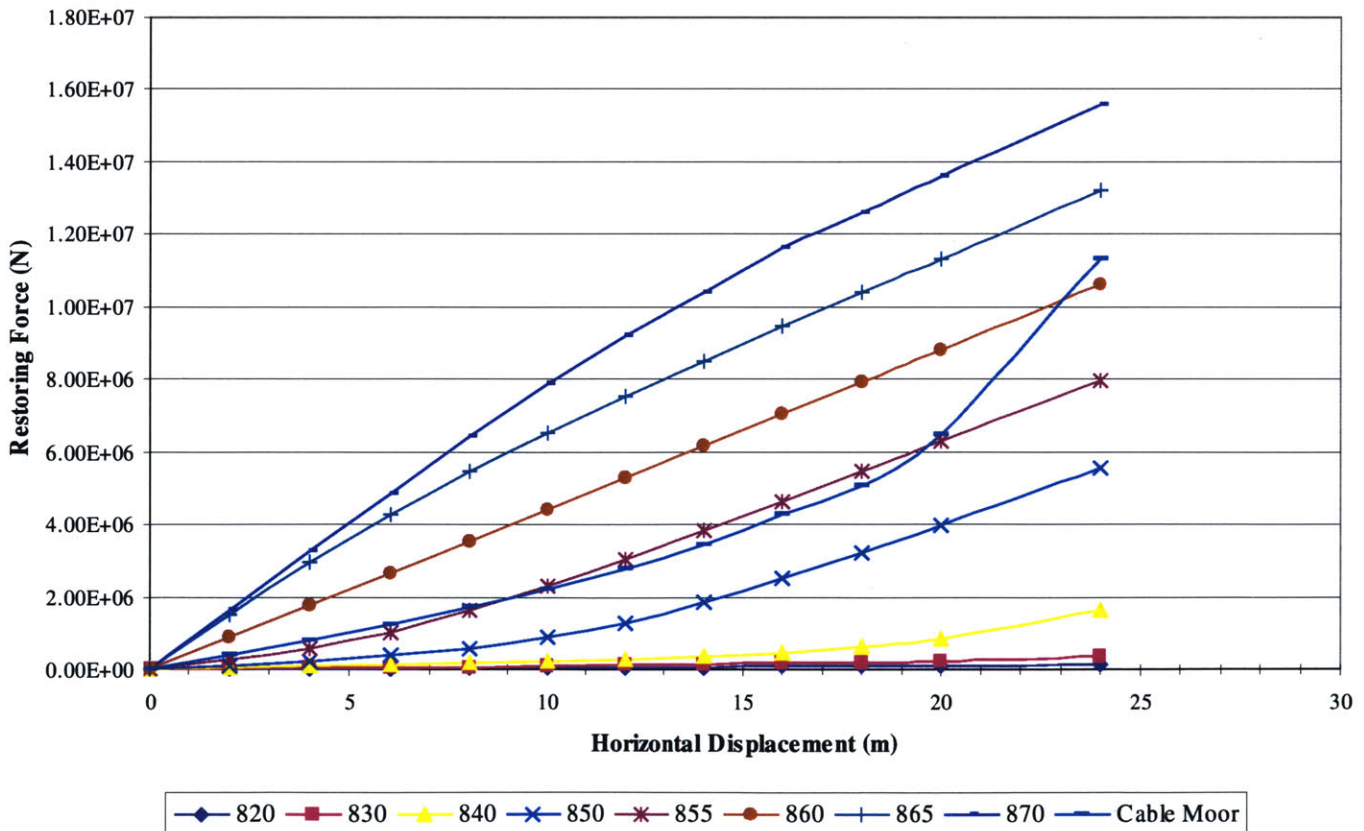


Figure 3-5: Moor static restoring forces

The previous graph shows the restoring force reaction to horizontal displacements out of the platform equilibrium position for all the initial configurations of synthetic mooring systems that were tested. Note that while the static response of the synthetic configurations is, in general, linear with respect to the displacement, that is not the case of the cable-type moor. The cable moor seems to have a linear behavior for small offsets from the origin, but as soon as the range is larger than 15 meters, the restoring force ramps up dramatically. The reason for this difference lays in the shape and weight of the different lines. For the light synthetic mooring lines, the mooring system needs to be taut in order to provide the required restoring. That is not the case of the cable configuration. Figure 3-3 shows that the cable lines are shaped in an arch way rather than in a straight line. Therefore, for small displacements of the platform from the origin, the moor will still have a loose pattern. However, as soon as the distance of the platform from its equilibrium position begins to increase, the cable lines become very taut. The restoring force they create in that case increases largely since they will then behave as a spring with very large Young modulus. The result of this phenomenon is a steep increase in the combined restoring force of all, 14, lines.

On the other hand, synthetic lines are very light compared to the cables. Hence, weight is not enough to provide the initial tensions that will fix the platform in its place if their initial disposition is as the one seen for the cable type moor. Note from figure 3-5 that only the three synthetic moors with highest pretension have a sufficiently large restoring force. Figure 3-4 also shows that all these three configurations are in the range of linear elastic behavior and thus, the three of them share an initial taut disposition. In other words, in order to achieve restoring forces comparable to those of the cable moor, the synthetic mooring systems need to have an initial taut configuration.

The following table shows material properties and the initial geometric conditions of the final tested synthetic lines. As mentioned before these configurations have a restoring force response that surpluses the one provided to the platform by the cable solution. Note

that the three different configurations only differ in the initial distance of all the anchors to the vertical of the floating body.

Catenary-type mooring line configuration (For each line)	Low Tension	Medium Tension	High Tension
Fairlead Depth	106.7 m	106.7 m	107.7 m
Hztal. dist. From Fairlead to Spar vert. axis	18.59 m	18.59 m	18.59 m
Anchor Depth	789.4 m	789.4 m	789.4 m
Hztal dist. From Anchor to Spar vert. axis	860 m	865 m	870 m
Total Line Length	1082 m	1082 m	1082 m
Pretension at Fairlead	$5.32 \cdot 10^5$ N	$1.11 \cdot 10^7$ N	$1.82 \cdot 10^7$ N
Weight in water (per unit length)	93 N/m	93 N/m	93 N/m
Weight in air (per unit length)	362 N/m	362 N/m	362 N/m
Diameter	0.2324 m	0.2324 m	0.2324 m
EA	$2.05 \cdot 10^8$ N	$2.05 \cdot 10^8$ N	$2.05 \cdot 10^8$ N
Added Mass Coefficient	1	1	1
Viscous drag Coefficient	1.2	1.2	1.2
Viscous Friction Coefficient	0.03	0.03	0.03

Table 3-3: Synthetic moor line's properties

These properties belong to a polyester synthetic cable. For a full table of material properties of synthetic ropes, see Appendix A. This specific material was chosen among all the possibilities shown in appendix A for several reasons. The polyester fiber was preferred over the aramid because it is softer, provides a smoother tension reaction and a bigger elongation for the same unstretched length. There are also economic issues when considering between these two solutions. In general, aramid fibers are more expensive than polyester. Among the polyester ropes, the one with the maximum diameter was elected because it had the maximum breaking strength.

The aspect of the whole synthetic mooring system is shown in the next figure:

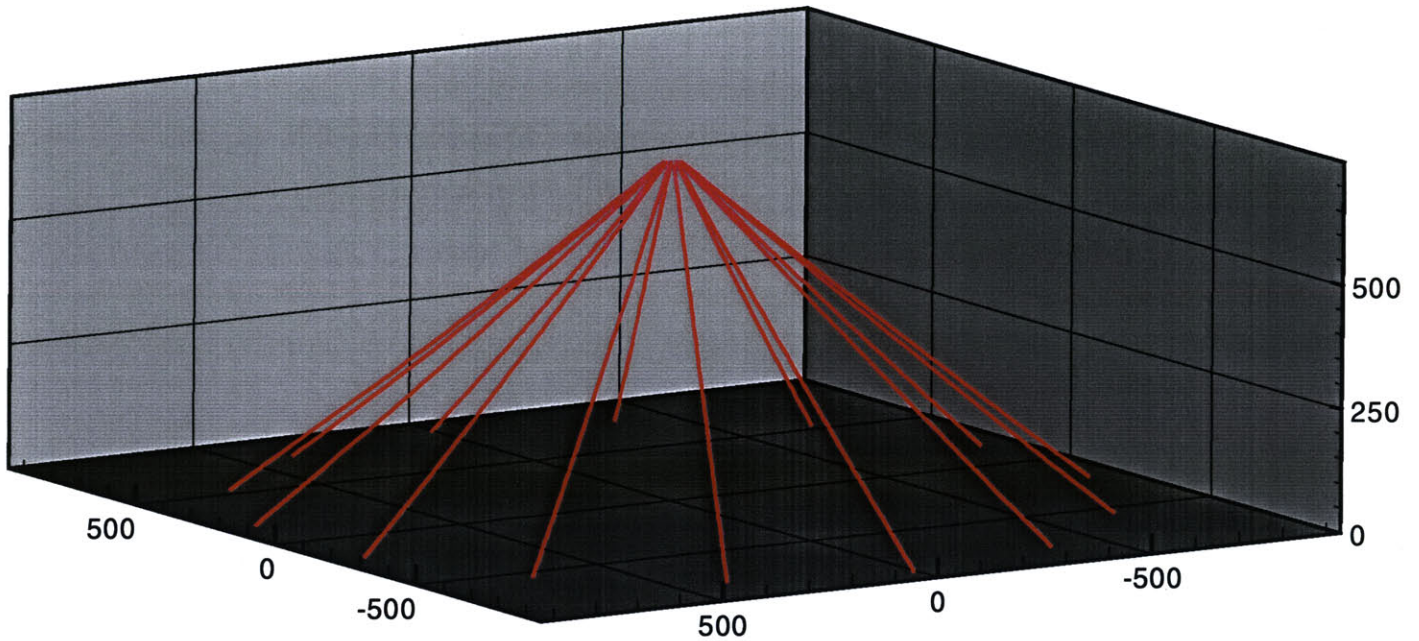


Figure 3-6: Synthetic mooring system

This last figure shows that even at an equilibrium position, the synthetic cables are shaped as straight lines. For the 3 synthetic mooring systems examined in this study, the shape looks the same and the only difference among them is the distance of the anchor and the consequent different rate of strain since all the lines have the same unstretched length.

This initial taut shape of the lines explains why the static force response of these mooring systems to offsets is linear. Provided that the tension in the lines does not reach ranges close to their breaking strength, the strain behavior of these synthetic ropes can be assumed as linear with respect to the internal tension in the lines. Given then, the initial taut disposition of this type of moor, it is expected for the static restoring force response not to show the non-linearities that the cable mooring system shows.

CHAPTER 4:

NUMERICAL RESULTS.

4.1. Comparison of the dynamic properties of the four moors

As mentioned in the second chapter, any floating body can sustain motions in 6 different directions. For the specific case of a SPAR platform held by means of a mooring line three of these motions are of special interest; surge, sway and heave. In the particular case of the first two, we can expect an axisymmetric behavior around the vertical axis due to the large number of lines and their specific disposition around the platform. Hence, only horizontal motions along the X-axis have been studied.

As also mentioned in the second chapter, when dealing with wave induced motions in floating bodies, there has to be a clear distinction among, linear and non-linear effects. Heave motions are fundamentally induced by wave linear effects, while in the surge direction, both linear and non-linear effects are important. Linear effects excite platform motions of amplitude in the same order as the amplitude of the waves that induce them, while the amplitude of the oscillations induced by slow drift effects are much larger. The natural periods of these two types of oscillations also differ a great deal, the natural period of the linear induced motions are also in the same order of that of the waves that

excite them. On the other hand, the natural periods of oscillation induced by slow drift effects are very long, typically in the order of one minute to a hundred seconds.

4.2.Slow Drift Oscillation:

The value of the maximum amplitude of oscillation induced to the platform due to slow drift effects is known, at least for the cable mooring system. From this maximum excursion and using information from figure 3-4 the value of the maximum excursions for different mooring systems is obtained. The taut synthetic moors should incur in smaller offsets since the restoring forces of the synthetic lines are larger for the same displacement.

To study the dynamic responses of the different mooring systems to drift excitations and to be able to compare the results, I have used the equivalent excursion for the synthetic moors. These equivalent excursions are calculated using as a base the static restoring forces of the cable mooring system and comparing them with the forces exerted by the 3 synthetic moors. The equivalent excursions for each system are displayed in the rows of the next table:

Equivalent Excursions (m)

Cable Mooring system	Synthetic. Low tension	Synthetic. Medium tension	Synthetic. High tension
10	6	4	4
15	10	5	5
20	14	9	8
25	25	20	16

Table 4-1: Equivalent excursion for slow-drift motions

These set of amplitudes have been studied for three different periods. These periods are 50, 100 and 150 seconds. Each of these mooring lines slow drift dynamic response has been tested for these 3 periods as well as their respective amplitudes of oscillation.

In order to be able to compare the damping energy loss among the four different mooring systems the damping results have been non-dimensionalized. The energy loss obtained from LINES 1.1 has been divided by the amplitude of the oscillations, the total mass of the platform and gravity. By using this non-dimensionalization the energy loss associated

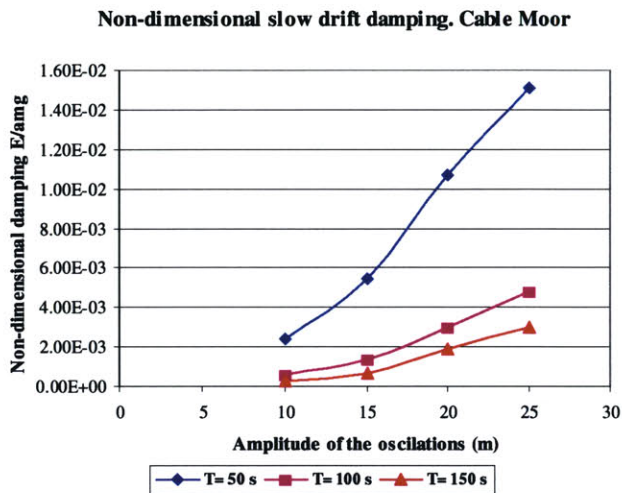


Figure 4-1: Slow drift damping. Cable.

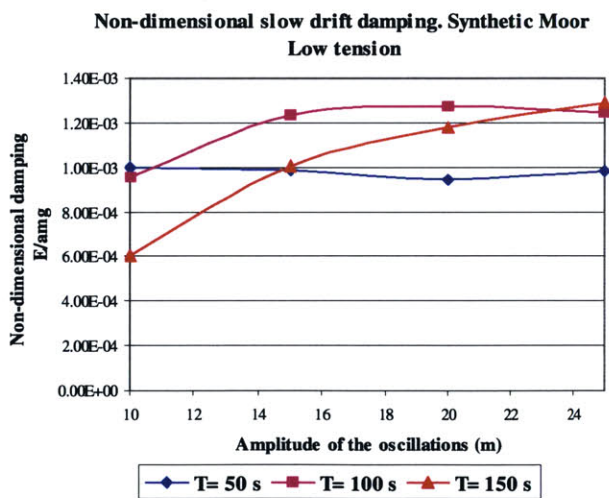


Figure 4-2: Slow drift damping. Synth. Low tension.

periods mentioned before.

to each equivalent motion can be compared with its equivalent in a different mooring system. The denominator of the non-dimensional damping represents the energy that the platform acquires when forced into oscillatory motions. The non-dimensional damping represents then the fraction of this energy that is absorbed every cycle by the mooring system.

The energy loss or damping for all the mooring systems are shown in the next set of figures, 4-1 to 4-4. In these figures, the general behavior of the damping in the different mooring systems has been plotted. These figures represent how the non-dimensional damping coefficient varies with the amplitude of the motion for the three distinct

Figure 4-1 shows the resulting damping for the cable mooring system, while the other three plots show the damping results for the synthetic cases, starting with the low tension graph, figure 4-2 and finishing with the high tension one, figure 4-4.

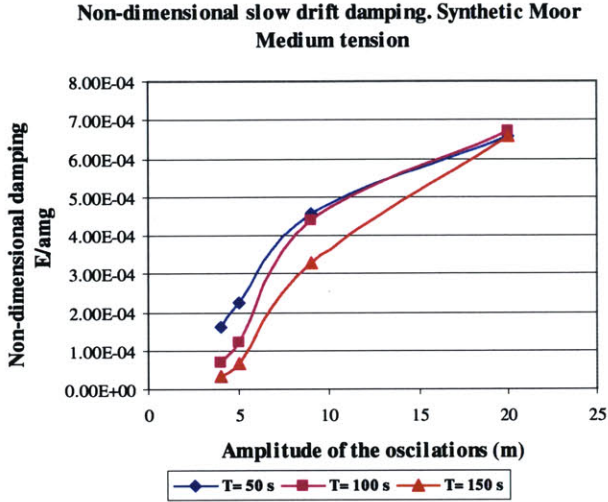


Figure 4-3: Slow drift damping. Synth. Medium tension.

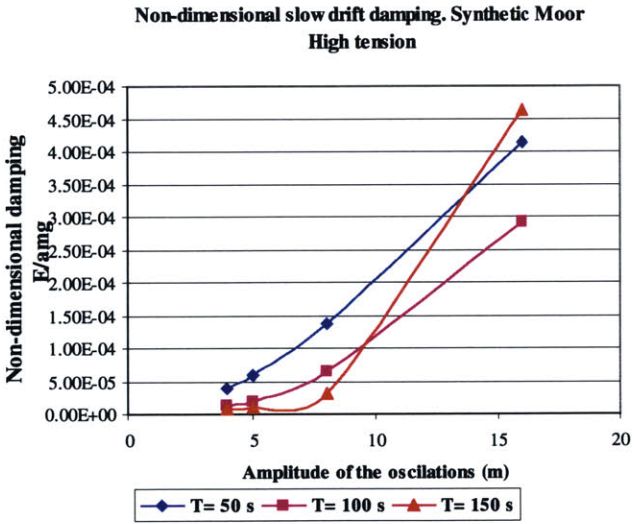


Figure 4-4: Slow drift damping. Synth. High tension.

The behavior of the damping coefficients in these graphs follows, up to some point, the expected shape. From these graphs we see that as the amplitude of the motions increases, so does the amplitude of the coefficient. The first of these graphs, 4-1, represents the cable catenary-type mooring system. From this graph, we notice that the smaller periods the larger the damping becomes. The reason for this behavior is that for a similar amplitude, as the period of oscillation decreases, the faster the velocities and accelerations of the line segments increase. The viscous and inertial terms in the governing equation become, therefore, very

crucial for two reasons. The first reason is the large weight of this line, considerably larger than the synthetic one, makes the inertial effects very important. The second affects the viscous terms of the governing equation. The transversal fluid-segment

relative velocity for the cable case is important due to the catenary like shape of the mooring lines. This increases the relative significance of the viscous terms.

In the remaining three graphs, we can also encounter the growth behavior of the non-dimensional damping as the amplitude of the oscillations is augmented. Note that the studied range of amplitudes for the synthetic cases varies and is smaller than the previous cable case. As previously stated, the reason for this modification is that the synthetic lines generate the same restoring forces for smaller excursions, given its initial taut disposition.

However, for these three cases the behavior of the non-dimensional damping regarding the period of the oscillations is different than the one seen in the cable mooring system. In these experiments, it is not always true that for a given amplitude, the smaller the period the larger the damping. Due to the initial taut shape of the mooring lines, the horizontal oscillations of the fairlead do not considerably modify the shape of these lines, which maintain, even under oscillations their straight-line shape. Rather, these horizontal oscillations modify the rate of strain in the lines.

Under this pattern of motion, the relative transverse velocities are rather small. This fact diminishes the importance of the viscous effects. The inertial effects are also of minor consequence compared to those of the cable moor since the density of the synthetics is by far smaller than the cable. Under these two assumptions the dynamic response of the mooring systems becomes very close to the static behavior. Therefore, the static responses of the lines become of considerable influence in these cases. As a result of the new relative significance of the static effects, the damping differences with a varying period become very small. Note then that, the range of the non-dimensional damping for the synthetic cases is lower than that for the cable moor case.

This last point regarding the range of the results in the damping coefficients becomes salient when we plot the results for a single period and all the four mooring systems in the same plot. The cable, being 10 times heavier than the synthetics, presents a higher variability of the damping due to modifications of the period than the rest of the

considered moors. The next two figures, 4-5 and 4-6, show the values of the non-dimensional damping for harmonic oscillation simulations with periods of 50 and 100 seconds. They show the resulting damping for all the different mooring systems.

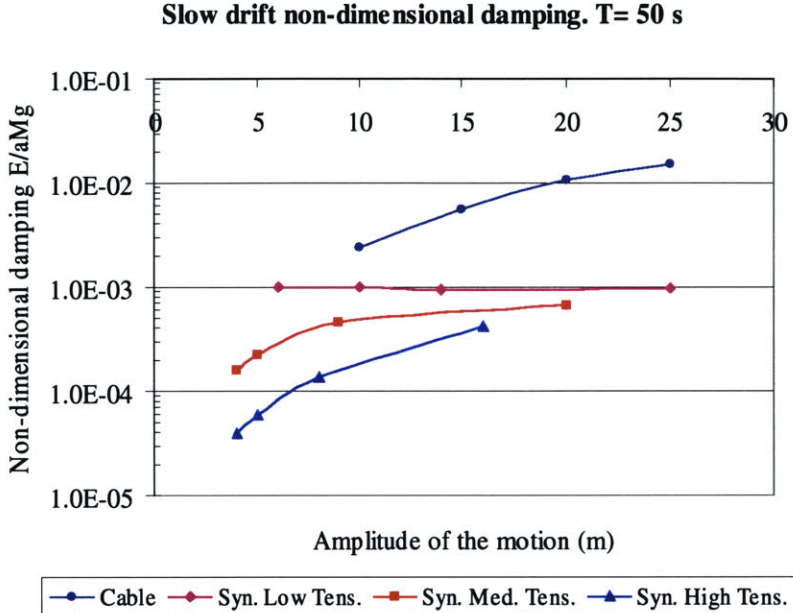


Figure 4-5: Slow drift damping. Period 50 s.

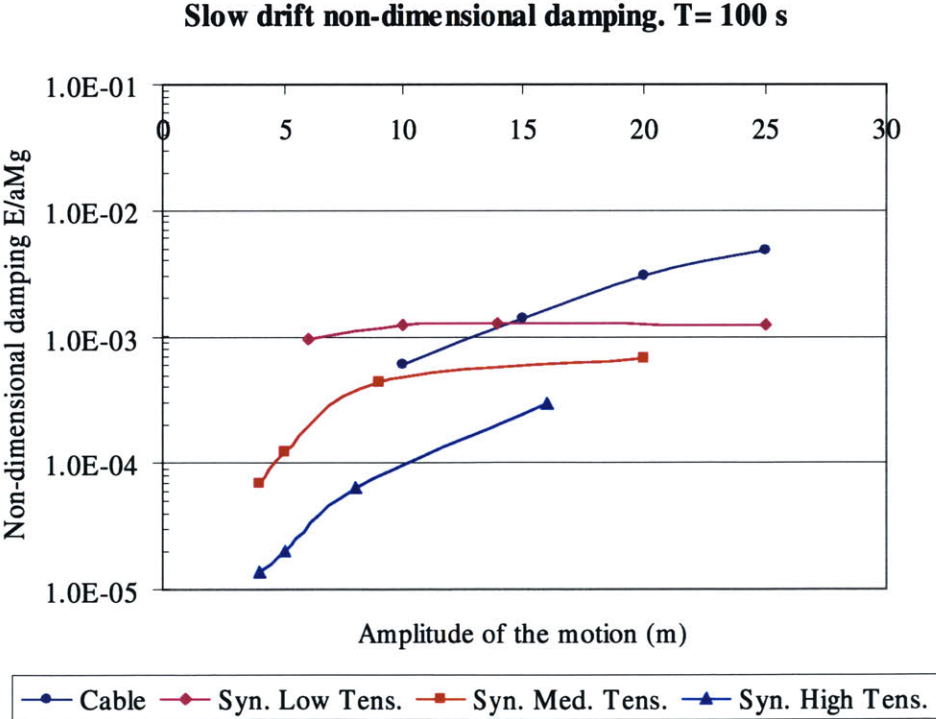


Figure 4-6: Slow drift damping. Period 100 s.

The plots in the previous page, 4-5 and 4-6, show that for “high” frequencies in the slow drift motions, the larger inertial effects of the cable mooring system create a large disparity in the outcome damping of the mooring lines. Remember that due to the equivalent excursion, an oscillation of amplitude 10 m. with the cable moor must be compared with the 4 m. amplitude motion in the case of synthetics under high pretension. Taking into account this aspect, the jump of non-dimensional damping from the original cable solution to the synthetic moors with highest pretension can almost reach two orders of magnitude.

The lower pretension synthetic mooring system presents much better damping qualities than the other two, at least regarding slow drift motions. The relative damping achieved by the original cable solution is typically bigger than that achieved by the low-tension synthetic moor, yet the differences are not as important. Moreover, when the oscillations became slower, and the inertial contributions are not as important, the damping attained by the low-tension synthetic moor turns out to be even larger than the cable solution. This is the result of a decrease in the damping of the cable moor when dealing with very long periods, rather than an increase of the damping in the synthetic solution. When the period of the oscillation becomes so long, we could even consider studying the damping using a quasi-static solution.

These considerations are clearly shown in the next pair of figures that represent the hysteresis cycles for oscillations of amplitude 10m, for cable, or the equivalent values for synthetic lines. The periods represented in figure 4-7 and figure 4-8 are fifty and one hundred seconds respectively. Note that the shape and most importantly the area of the hysteresis cycles of the synthetic solutions do not change noticeably from the first to the second figure.

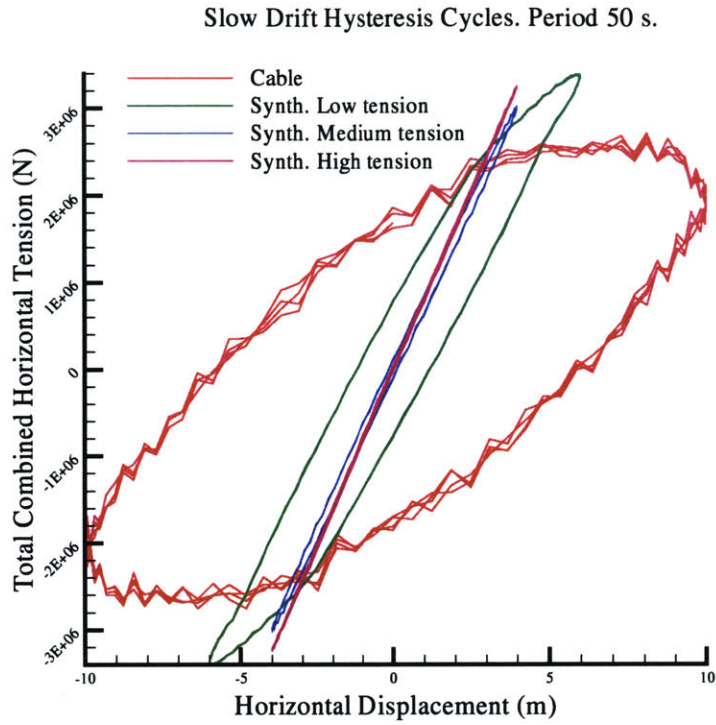


Figure 4-7: Slow drift hysteresis Cycles. Period 50s.

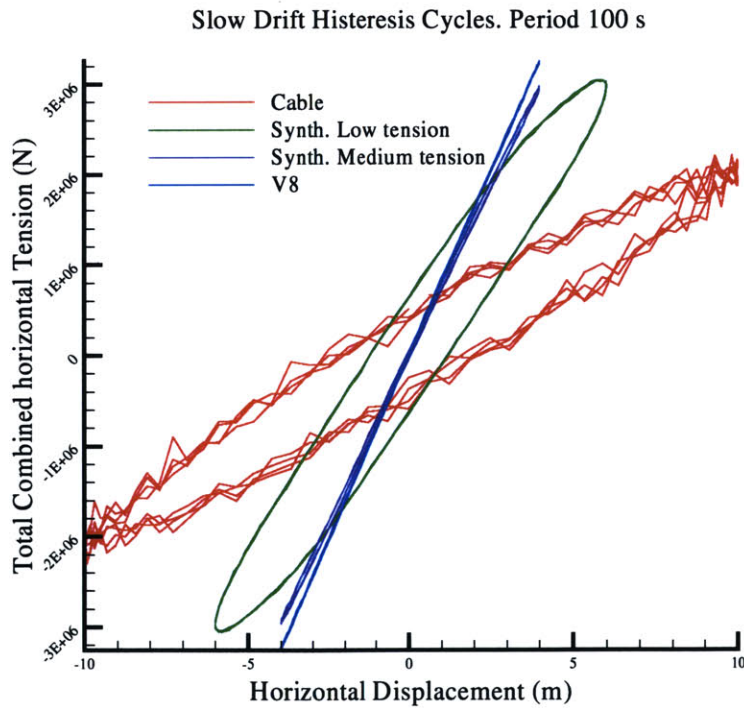


Figure 4-8: Slow drift hysteresis Cycles. Period 100s.

On the other hand, the hysteresis loop of the original cable solution suffers a noticeable area decrease when the period goes from 50 seconds to 100 seconds. The shape of this loop turns thinner as the frequency of the oscillation decreases and it appears more like the static or quasi-static response. The 100 seconds period cycle for the cable mooring system tends to a series of quasi-static solutions of the mooring system's restoring forces because the period of oscillation is very long.

These graphs, 4-7 and 4-8, also show why the damping of the two synthetic lines with higher pretension is so small. It is important to notice that due to the high tension and the initial taut conditions, they behave almost like springs providing very little slow drift damping to the floating structure. These two moors are relatively insensitive to the period variation, at least in this range of motions. The reason for this is that they already behave as a linear quasi-static system for the smaller period, so increasing the length of the period cannot force them to lose any more area in their associated hysteresis cycles.

The low-tension synthetic system, also, presents very little modification in its area due to the variation in the period of the motion. The result displayed in figures 4-7 and 4-8 for the low-tension synthetic damping looks counter intuitive because the 50 seconds hysteresis loop presents sharper ends than the 100 seconds loop. The most probable reason for this is that the faster oscillation induces higher fairlead tensions of the moor on the extremes of the cycle. As a result of these higher tensions, the mooring system reacts quicker, sharpening the extremes of the hysteresis loop.

The range of the forces is very similar for all the cases proving that the initial consideration of the equivalent excursion is accurate. The dynamic reaction of the moors does not introduce, in the slow drift case, a big enough modification in the tensions for a reconsideration of the equivalent excursion hypothesis.

Finally, note that the excursions are variable, and each mooring system range of displacements is different. In this context, the responses with lower motions have to lose less energy because the platform, principal mass of the whole linear system, is also undergoing smaller oscillations and therefore presents less motion energy.

4.3.Linear Surge Oscillations

For the linear surge oscillations of the mooring lines I followed a similar procedure to the one performed in the slow drift motion. All the different mooring systems were tested for various horizontal amplitudes under a range of periods similar to those of regular waves in deep water areas.

In order to compare the damping results from the different mooring systems, I used again the same non-dimensional damping quantities, dividing the original energy loss by the weight of the platform in Newtons and the amplitude of the oscillation.

Regardless of the range of amplitudes studied for each of the mooring systems all of them have been tested under the same collection of motion periods. For the linear surge oscillations the periods considered are 7, 10 and 15 seconds. Each moor has been studied for all of these periods and a range of amplitudes starting at values as small as half a meter and up to oscillations of three meters wide. The range of amplitudes used for each mooring system is displayed in the next table:

Amplitudes studied for each mooring system. All in meters.

Cable Moor	Synth. Moor. Low Tension	Synth. Moor. Medium Tension	Synth. Moor. High Tension
1	0.5	0.3	0.3
2	1	0.6	0.6
3	1.5	0.9	0.9
	2	1	1
	3	2	2
		3	3

Table 4-2: Linear surge amplitudes

The concept of equivalent excursion has not been used for linear oscillations. The frequency of these harmonic motions is much faster than the slow drift case. Now, the dynamic effects in the internal tension are considerable. The maximum tensions involved in these oscillations are higher than the static restoring forces that would result from a similar platform displacement. The dynamic effects are very influential in the case of the cable mooring due to its heavy weight. Therefore, if we tried to use equivalent excursions, we would find that the forces involved in the existent cable moor would be much higher than those that would appear in the case of synthetic mooring systems. The meaning of equivalent excursion would disappear since the range of tensions involved in two “equivalent” oscillations would be different.

The results of the linear surge damping experiments are displayed in the next set of figures, 4-9 to 4-12. Each moor configuration is shown in a different graph. These graphs show how the damping for different period series vary with the amplitude of the motion.

Figure 4-9 demonstrates the damping behavior for the cable mooring system. As expected, the damping increases with the amplitude and frequency of the motion. Figures 4-10, 4-11 and 4-12 represent the synthetic cases for low, medium and high initial tension. These three other figures display the same behavior with regard to the amplitude of the oscillations. The larger the amplitude of the oscillation is, the larger the equivalent

damping coefficient. The variation of the damping with regard to the period of

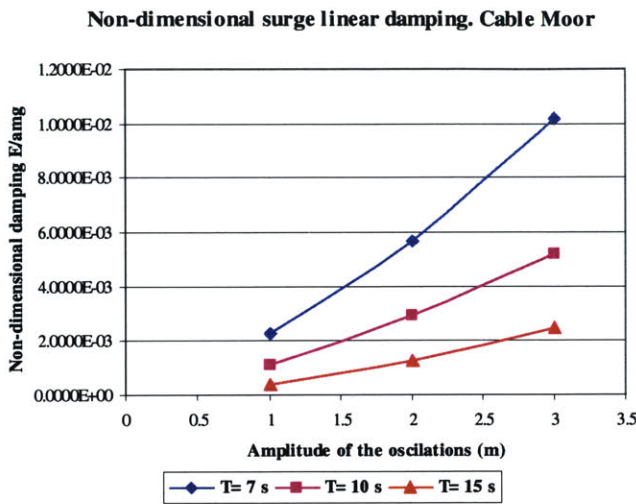


Figure 4-9: Linear surge damping. Cable.

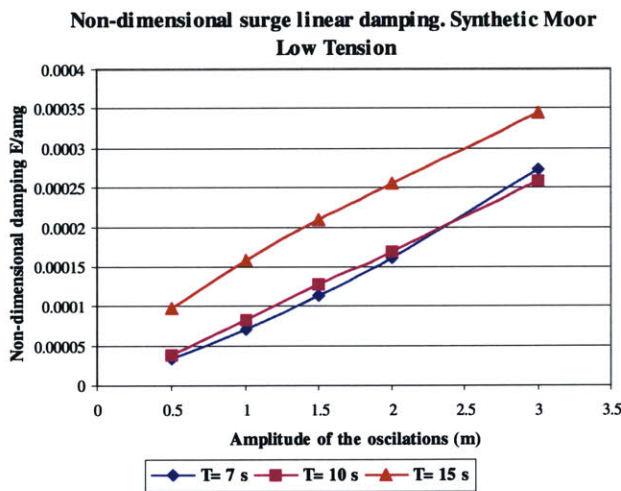


Figure 4-10: Linear surge damping. Synth. Low tension

oscillations does not have such a clear pattern for the synthetic cases as the one presented in the cable case.

The energy loss behavior with the period variation does not show a common blueprint for the three synthetic cases. In the case of the lower tension, the higher periods show larger damping. The medium pretension synthetic case shows a behavior where the higher the frequency, the higher the damping. And finally, the high pretension synthetic solution shows that the largest damping corresponds to the period of ten seconds.

The reason for this behavior might be hidden in the mooring line configuration. Note that these oscillations are relatively small compared to the dimension of the lines, and that the synthetic mooring systems are taut. Under those initial conditions, the lines in the moor whose direction is aligned with the direction of motion, are going to experience very little movement. Moreover, these motions are going to be mainly in the direction of the lines themselves, modifying the stretch degree of the line but not creating any added mass or viscous effects.

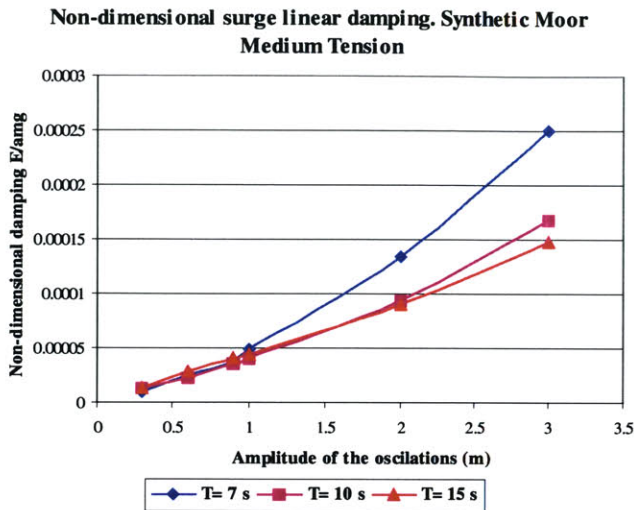


Figure 4-11: Linear surge damping. Synth. Med. tension

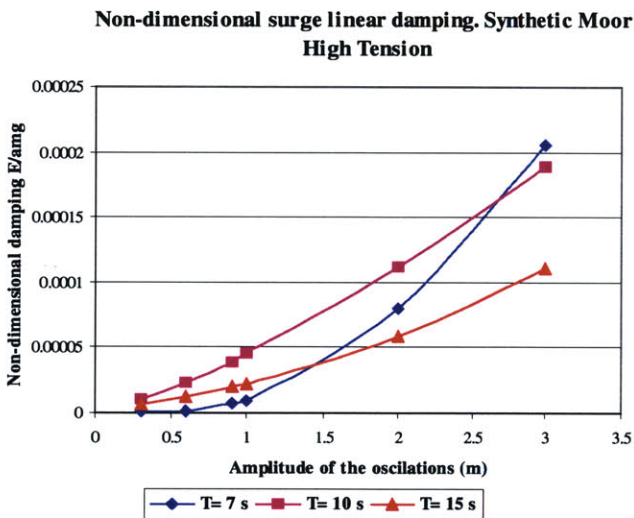


Figure 4-12: Linear surge damping. Synth. High tension

figure 4-13. Again this plot reveals that, as for the slow drift motion, the cable configuration provides at least ten times more energy absorption than the best synthetic proposition.

The creation of non-linear viscous effects that govern the damping in the taut mooring cases are then accomplished mainly by the lines whose direction is transverse to the direction of the motions.

The pretension of these lines dictates the way they behave relative to transversal oscillations of their fairleads. Depending on this pretension they will react differently to the diverse periods of oscillation, and therefore explain the appearance of a priority as well as the odd behavior of the damping patterns.

The damping results for horizontal oscillations of ten seconds period and all the moor configurations are shown in

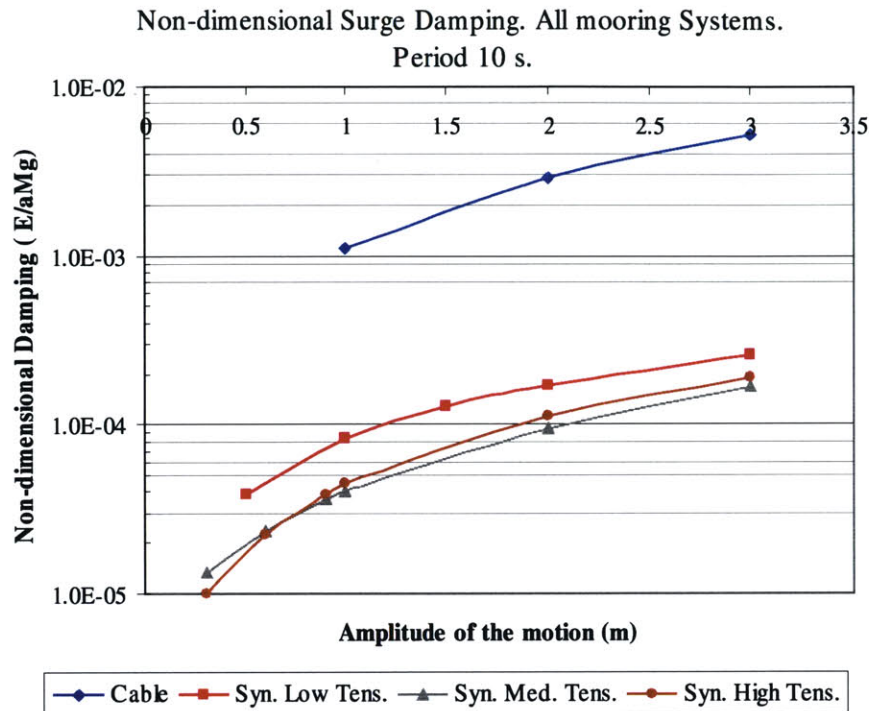


Figure 4-13: Linear surge damping. Period 10 s.

This figure also shows that the difference among the various synthetic solutions is very small, especially for the higher initial tensioned mooring systems.

Note also, that the linear surge damping for all the moor solutions shows an almost exponential behavior with respect to the amplitude of the motions.

The explanation for the dramatic jump in damping for the cable solution lies in the hysteresis loops of these four mooring solutions. The hysteresis loops for a motion of seven and fifteen seconds periods and amplitude of three meters are plotted in figures number 4-14 and 4-15. Following the same trend as the slow drift hysteresis loops, the cable configuration cycle encloses a much larger area than the synthetic solutions. The cable hysteresis loop is very sensitive to variations of the oscillatory period, while the synthetic moors show again a quasi-static response with unremarkable effects.

Linear Surge Hysteresis Cycles. Period 7s

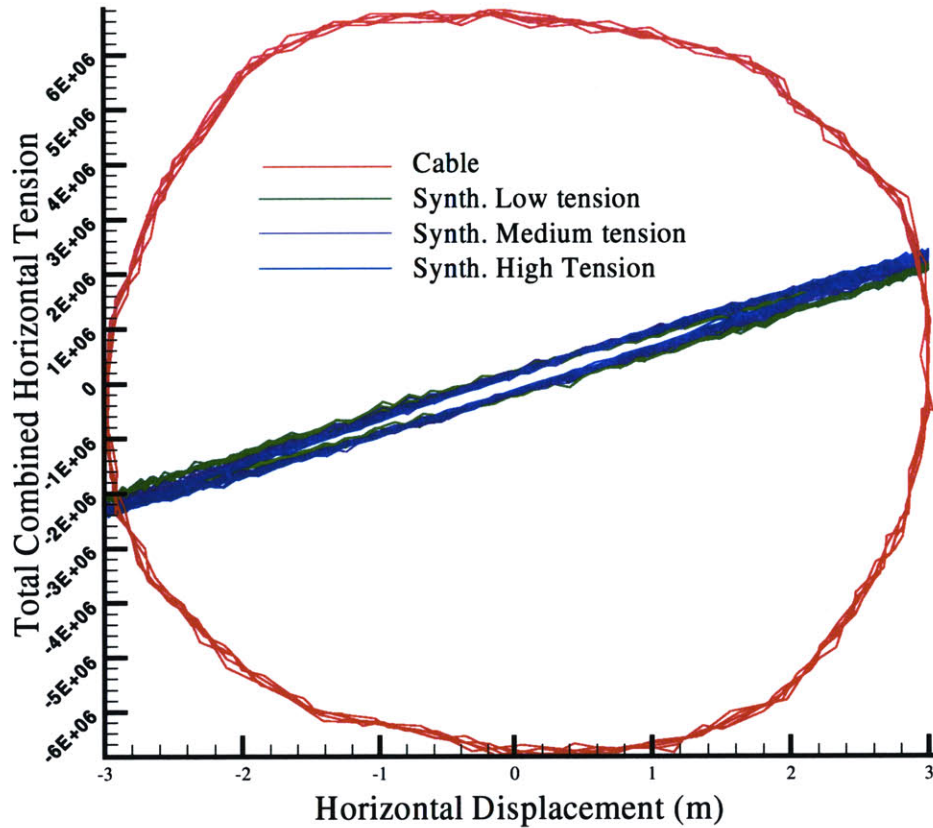


Figure 4-14: Linear surge hysteresis cycles. Period 7s.

These two figures, 4-14 and 4-15, show that the maximum values of the forces involved in the motions are larger for the cable moor than for the synthetic ones. This result proves that the notion of equivalent excursions does not apply for linear motions. If we had wanted to ensure the maximum forces to be the same magnitude for all the mooring systems, the excursions of the platform for the synthetic moors should have been larger than their equivalent for the cable moor.

Linear Surge Hysteresis Loops. Period 15s.

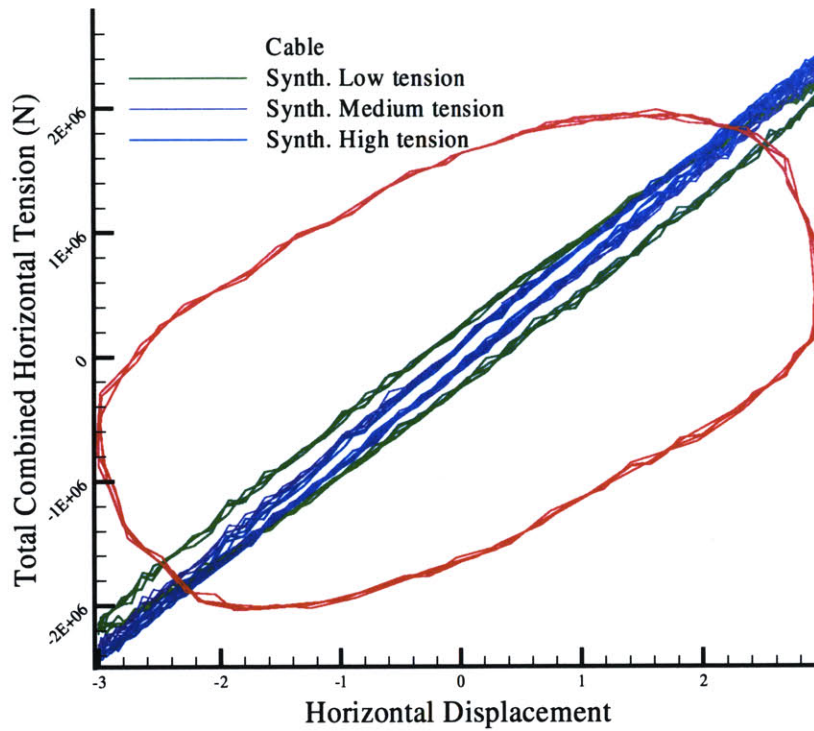


Figure 4-15: Linear surge hysteresis cycles. Period 15s.

4.4. Heave Oscillations

The same procedure that I have used to study the last two cases is going to be followed in this section for the damping responses of the moorings to the heave oscillations. Given the cylindrical shape of the platform and its depth, the excitation in heave has a smaller intensity than the excitations in surge or sway. This smaller excitation force leads to smaller oscillations of the platform in the vertical mode than that achieved in the horizontal direction.

For this mode of oscillation, all the platforms have been tested under the same set of conditions. The range of periods used for these experiments has been the same as those in the linear surge motions: seven, ten and fifteen seconds. Being both linear surge and

heave oscillations induced by first order interactions, their respective motions would also present similar frequencies. The amplitudes of the heave harmonic motions are smaller

than those used for linear surge. These experiments have been carried out varying the amplitude of the motions among the following values: 0.5, 1 and 1.5 meters.

The results for this set of experiments are displayed on figures 4-16, 4-17, 4-18 and 4-19. These figures show the particular behavior of each mooring line damping with respect to the amplitude of the motions. Series are separated as in the previous cases by period of the oscillation.

The same behaviors, as found in the first two sets of experiments, also exist regarding the modification of the absorbed energy and its relation to the increased amplitude of the motion increases. All the mooring systems show that the larger the amplitude, the larger the damping for a given frequency of the motions.

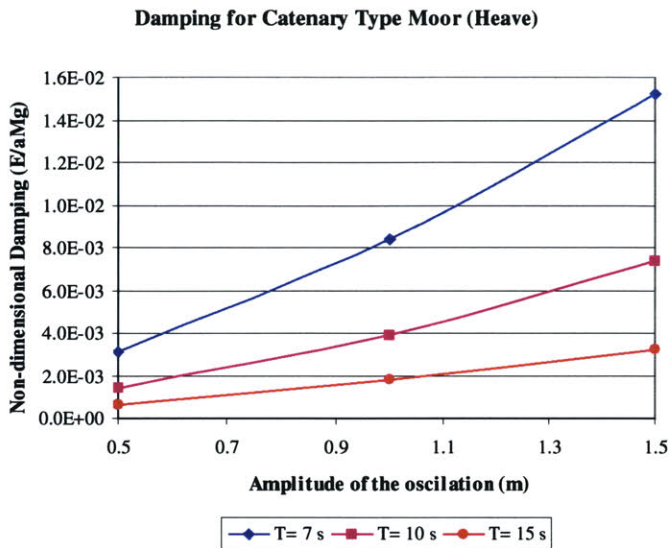


Figure 4-16: Heave damping. Cable.

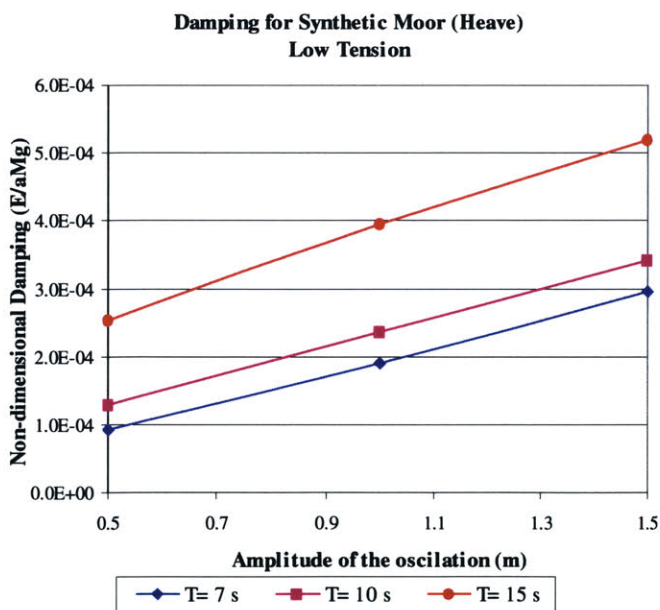


Figure 4-17: Heave damping. Synth. Low tension.

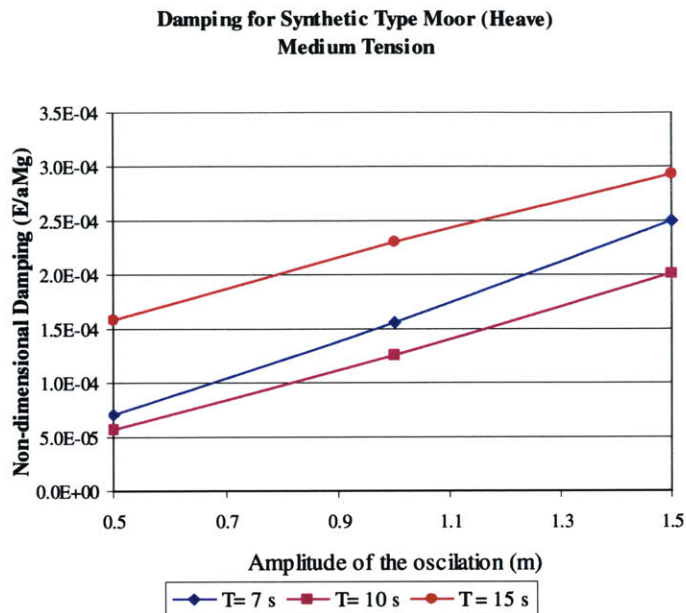


Figure 4-18: Heave damping. Synth. Medium tension.

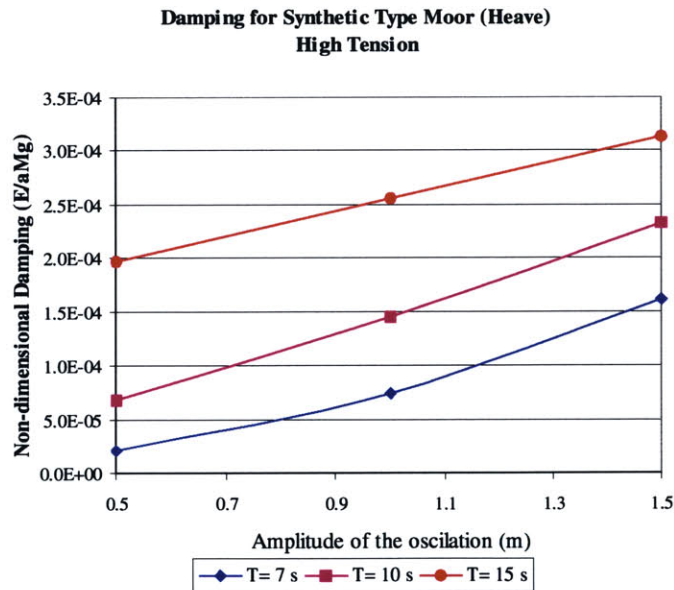


Figure 4-19: Heave damping. Synth. High tension.

Regarding the behavior of the damping coefficients with respect to the period of the oscillations, the same results as in the previous experiences are found. The cable moor clearly shows that the damping grows as the frequency of the oscillation increases. On the other hand, the synthetic moors do not seem to present a clear pattern of behavior when the period of the oscillation varies.

All the three synthetic solutions present their highest damping under the fastest oscillation of the fairlead. Again, this result might seem counterintuitive and it probably falls under a similar hypothesis mentioned in the linear surge case. All the lines are now forced to move in a direction transverse to their tangential axis. The vibration of each line will depend on the initial pretension and the period

of oscillation of the fairlead. Should any of the periods induce an oscillation close to resonant motion of the line, the viscous effects would ramp up in the process creating a new large damping.

Figure 4-20 compares the damping coefficients for all the mooring solutions under a period of ten seconds. Again, the cable configuration shows an energy absorption that is over one order of magnitude larger than the damping achieved by any of the synthetic solutions. In addition, the low-tension synthetic solution presents again the largest damping of all the taut mooring systems.

But not all are similarities, figure 4-21 shows the hysteresis loops of the different solutions for a period of ten seconds and an amplitude of one and a half meters. This graph displays very clearly that each mooring system has different initial pretensions. Due to this difference, the range of tensions encountered for each moor loop is shifted vertically from each other. In the case of horizontal directions the axisymmetric disposition of the lines would cancel out the total resulting force that the moor exerted into the platform. For the vertical case, all the lines are pulling down with an equal force and the compounded result is no longer void.

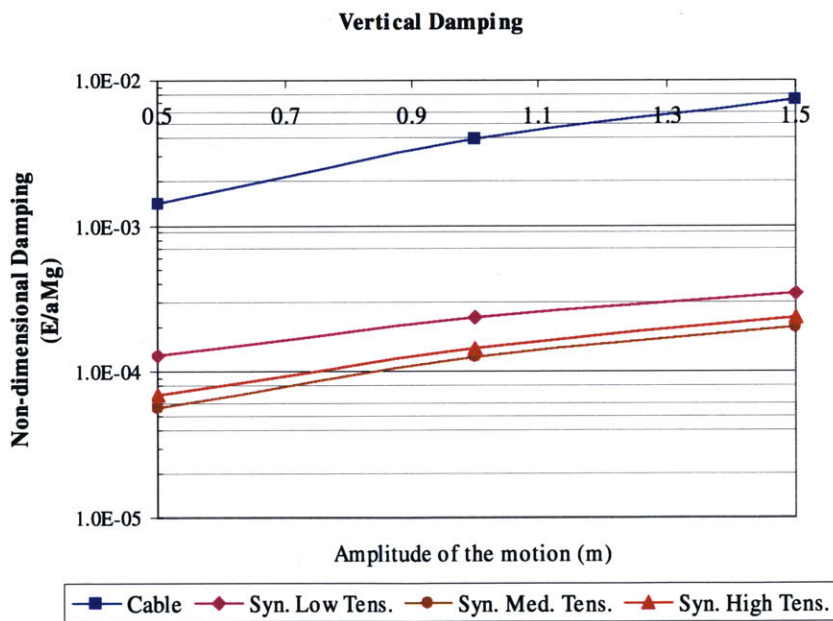


Figure 4-20: Vertical damping. Period 10s.

Heave Hysteresis Cycles. Period 10 s

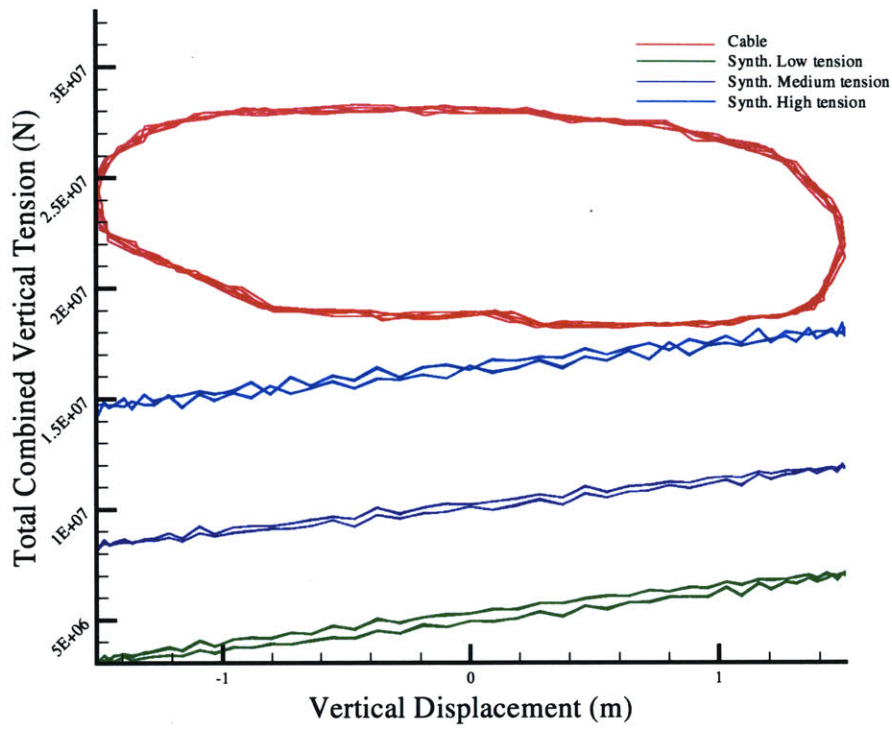


Figure 4-21: Heave hysteresis Cycles. Period 10s.

The difference in pretension of these moors would result in a modification of the platform's initial vertical position or the necessity to introduce into the platform a type of ballast. However, the equilibrium position would not be modified more than a meter and a half from the cable to the lower tension synthetic solution. Thus having left this initial consideration out of the tests does not introduce any important modification to the final results.

CHAPTER 5:

DAMPING RELATIVE IMPORTANCE

5.1 Linear Damped oscillator

To study the relative importance of the damping of different mooring systems, these results have been compared using a linear approximation. The idea is to compare all the results from the previous experiments using a simplification of formula 2.1. However, instead of using a coupled second order linear equation with six degrees of freedom, this approximation considers only motions in one dimension.

When formula 2.1 is reduced to one degree of freedom it yields to,

$$(m + a)\ddot{x} + b\dot{x} + kx = f \tag{5.1}$$

That corresponds to the next simplified mechanical system.

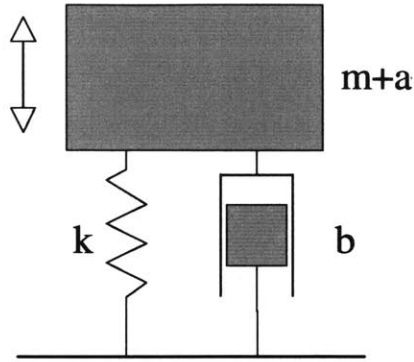


Figure 5-1: Simple model for damped oscillator.

Where “m+a” represents the mass of the oscillator plus its added mass, k is the coefficient of the spring and b is the linear damping of the system.

Now, dividing by the coefficients of the second order term and considering only the unforced oscillations, the equation can be rewritten as,

$$\ddot{x} + 2\sigma \dot{x} + \omega_o^2 x = 0 \quad (5.2)$$

Where sigma and the natural frequency of the system, ω_o , are defined as,

$$\sigma = \frac{b}{2(m+a)} \quad (5.3)$$

$$\omega_o = \sqrt{\frac{k}{m+a}}$$

This equation presents a close form solution that depends on the *damping ratio* of the system, ζ , that is defined as,

$$\zeta = \frac{\sigma}{\omega_o} \quad (5.4)$$

The damping ratio is an index of the stability of the system’s stability to non-forced oscillations, if ζ is negative, the system is unstable and the initial motion would grow

without bound. When ζ is zero, the system is just neutrally stable, and as the value of ζ increases towards 1, the relative damping of the system increases. For values of ζ larger than 1, the system will not overshoot the neutral position. For small values of ζ , the damping ratio indicates explicitly the number of cycles, n , to damp the amplitude of the oscillation to $1/e$ its original value. N is given by the next equation,

$$n \approx \frac{1}{2\pi\zeta} \tag{5.5}$$

The following figures show the system oscillation responses with time for a fixed starting position and different values of the damping ratio, ζ .

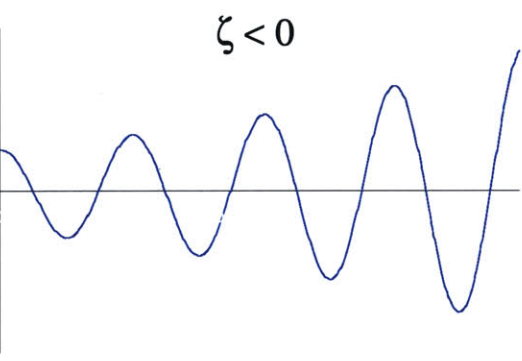


Figure 5-2.A: Unstable oscillation

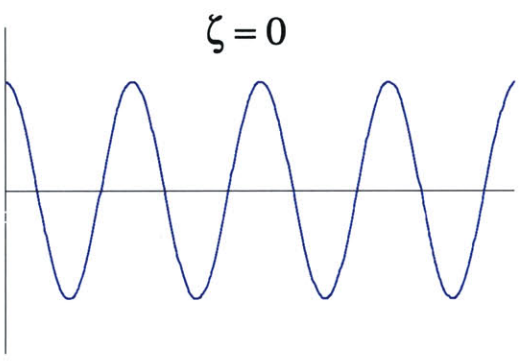


Figure 5-2.B: Neutrally stable

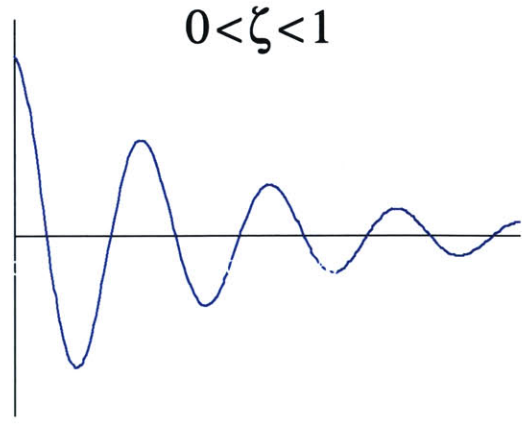


Figure 5-2.C: Damped oscillations

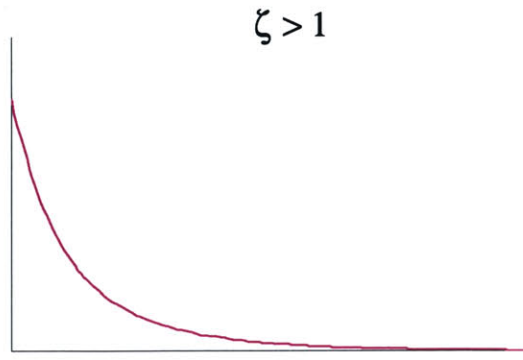


Figure 5-2.D: Collapse response

The approximation for the platform and moor group to a linear system will always be similar to the case of figure 5-2.C. The mass of the system is very large while the restoring and damping coefficients are in the same order of magnitude. This fact places the damping ratio in the bracket of zero to one.

5.2. Platform-moor coefficients

The approximation of the platform-moor group response to a linear system requires some simplifications in order to obtain coefficients for restoring and linear damping.

The first simplification is relative to the restoring force of the moor. According to the formula 5.1, the restoring force of the moor will only depend on the position of the platform. As we saw in the hysteresis loops, this will only be an approximation since the tension of the moor depends also on dynamic effects. The relative restoring forces must be transformed into a linear response mechanism. For this purpose, the static responses of the mooring systems have been used, ignoring all dynamic effects and their repercussions in the final tension.

In the case of the synthetic lines, this simplification is rather accurate since the inertial effects of the lines are not very significant. Also, their static response is very close to a straight line. For the case of the cable moor, the inertial effects are more important and the static restoring forces are not even linear. However, this approximation provides a very good general idea in order to compare the dynamics of the different solutions.

The second step to take towards the utilization of the equivalent system is to convert the energy loss per cycle into its equivalent linear damping coefficient, b in the linear equation 5.1. For this step, it is assumed that the instantaneous value of the internal tension on the line can be approximated by

$$T = b \frac{dx}{dt} \quad (5.6)$$

Now, combining formula 2.27 (in this case only for one dimension) with 5.6 we can obtain the relation between the energy loss per cycle obtained through a numerical simulation, and the linear damping coefficient that is needed for the linear approximation.

$$E = \int_t^{t+\tau} \vec{F}(t) \cdot \frac{dx}{dt} dt \cong b \int_t^{t+\tau} \left[\frac{dx}{dt} \right]^2 dt = b \frac{2\pi^2 a^2}{\tau} \quad (5.7)$$

Now, rewriting this equation we obtain the equivalent linear damping,

$$b = \frac{E\tau}{2\pi^2 a^2} \quad (5.8)$$

However, the linear damping results vary for different periods and amplitudes of the motion. The linear approximation requires a constant damping, so I have used the mean value of all the damping results as a definitive approximation to the linear mechanical system.

Slow drift surge, linear surge and heave, have been studied using separate linear approximations because the difference among the damping coefficients is rather large, and the character of the three modes of oscillations is very different. Even for only one of these modes of oscillation, the linear damping coefficient is far from being constant. Note in table 5-1 that the standard deviation of the mean linear damping coefficients are of the order of their respective averages themselves.

Regardless of these facts, the linear approximation still gives a very good sense of the dynamics of the platform with the different mooring solutions. They are only a first estimate, yet an improvement of these results would take a full numerical resolution of the differential equation using non-constant coefficients.

5.3 Linear Approximation

The coefficients obtained for the linear approximations are shown in the following tables. Each table presents one mode of oscillation and all four types of mooring solutions.

- Slow drift surge motions:

	Cable Moor	Synthetic. Low tension	Synthetic. Medium tension	Synthetic. High tension
Platform mass (kg)	$2.205 \cdot 10^8$	$2.205 \cdot 10^8$	$2.205 \cdot 10^8$	$2.205 \cdot 10^8$
Added mass coefficient	1	1	1	1
Total mass (kg)	$4.41 \cdot 10^8$	$4.41 \cdot 10^8$	$4.41 \cdot 10^8$	$4.41 \cdot 10^8$
Mean linear damping (Ns/m)	1635324	1015696	314303.11	110438.7
Damping stand. Deviation (Ns/m)	884022.8	532953.3	158680.2	124896.6
Restoring force (N/m)	295136	441139	585822	704499

Table 5-1: Linear approximation coefficients for slow drift motion.

- Linear Surge motions:

	Cable Moor	Synthetic. Low tension	Synthetic. Medium tension	Synthetic. High tension
Platform mass (kg)	$2.205 \cdot 10^8$	$2.205 \cdot 10^8$	$2.205 \cdot 10^8$	$2.205 \cdot 10^8$
Added mass coefficient	1	1	1	1
Total mass (kg)	$4.41 \cdot 10^8$	$4.41 \cdot 10^8$	$4.41 \cdot 10^8$	$4.41 \cdot 10^8$
Mean linear damping (Ns/m)	3405893	198982	77411.1	59125.6
Damping stand. Deviation (Ns/m)	2136281	152424	70169.5	65731.6
Restoring force (N/m)	295136	441139	585822	704499

Table 5-2: Linear approximation coefficients for linear surge motion.

- Linear Heave motions:

	Cable Moor	Synthetic. Low tension	Synthetic. Medium tension	Synthetic. High tension
Platform mass (kg)	$2.205 \cdot 10^8$	$2.205 \cdot 10^8$	$2.205 \cdot 10^8$	$2.205 \cdot 10^8$
Added mass coefficient	0	0	0	0
Total mass (kg)	$2.205 \cdot 10^8$	$2.205 \cdot 10^8$	$2.205 \cdot 10^8$	$2.205 \cdot 10^8$
Mean linear damping (Ns/m)	3405893	198982	77411	59125
Damping stand. Deviation (Ns/m)	2316281	152424	70169	65731
Restoring force (N/m)	$1.31 \cdot 10^6$	$1.28 \cdot 10^6$	$2.11 \cdot 10^6$	$1.84 \cdot 10^7$

Table 5-3: Linear approximation coefficients for linear heave motion.

Note that both surge motions share the same added mass coefficient, 1, equal that of an infinitely long cylinder. The length of the spar platform is large enough so that using 1 as added mass coefficient is a good initial value for the linear approximation. Meanwhile, the vertical motions of the platform added mass is zero. Only the water under the bottom of the platform is accelerated when the platform undergoes vertical oscillations. This volume of water, and especially its respective weight, is very small compared to the platform weight.

Also note that, the two horizontal modes of motion share the same restoring coefficients. All the restoring in this direction comes from the mooring system. On the other hand, when dealing with the motions in heave, the amount of water displaced by the platform must be considered. The restoring in this case comes from the contributions of the mooring lines and the buoyancy variation of the platform. For the cable moor and the low tension synthetic moor, most of the restoring force comes from buoyancy effects. On the other hand, for the two higher tension synthetic solutions, the mooring effects are as important as the buoyancy contribution.

Using the previous coefficients is straightforward to calculate the non-dimensional parameters and the damping ratio, ζ , that are needed for the linear approximation. The results for these coefficients are displayed in the following tables.

- Non dimensional coefficients: Slow drift surge.

	Cable Moor	Synthetic. Low tension	Synthetic. Medium tension	Synthetic. High tension
σ (1/s)	$1.854 \cdot 10^{-3}$	$1.1516 \cdot 10^{-3}$	$3.5636 \cdot 10^{-4}$	$1.252 \cdot 10^{-4}$
Natural frequency (1/s)	$2.587 \cdot 10^{-2}$	$3.1628 \cdot 10^{-3}$	$3.6448 \cdot 10^{-3}$	$3.996 \cdot 10^{-3}$
Natural Period (s)	242.8	198.6	172.4	157.2
Damping ratio, ζ	$7.16 \cdot 10^{-2}$	$3.6411 \cdot 10^{-2}$	$9.77 \cdot 10^{-3}$	$3.122 \cdot 10^{-3}$

Table 5-4: Linear approximation non-dimensional coefficients for slow drift motion.

- Non dimensional coefficients: Linear surge.

	Cable Moor	Synthetic. Low tension	Synthetic. Medium tension	Synthetic. High tension
σ (1/s)	$3.861 \cdot 10^{-3}$	$2.256 \cdot 10^{-4}$	$8.777 \cdot 10^{-5}$	$6.703 \cdot 10^{-5}$
Natural frequency (1/s)	$2.587 \cdot 10^{-2}$	$3.1628 \cdot 10^{-3}$	$3.6448 \cdot 10^{-3}$	$3.996 \cdot 10^{-3}$
Natural Period (s)	242.8	198.6	172.4	157.2
Damping ratio, ζ	$1.492 \cdot 10^{-1}$	$7.1332 \cdot 10^{-3}$	$2.4081 \cdot 10^{-3}$	$1.677 \cdot 10^{-3}$

Table 5-5: Linear approximation non-dimensional coefficients for linear surge motion.

- Non dimensional coefficients: Linear heave.

	Cable Moor	Synthetic. Low tension	Synthetic. Medium tension	Synthetic. High tension
σ (1/s)	$7.723 \cdot 10^{-3}$	$4.5122 \cdot 10^{-3}$	$1.75122 \cdot 10^{-4}$	$1.340 \cdot 10^{-4}$
Natural frequency (1/s)	$7.079 \cdot 10^{-2}$	$7.619 \cdot 10^{-2}$	$9.7823 \cdot 10^{-3}$	$2.888 \cdot 10^{-3}$
Natural Period (s)	81.5	82.46	64.23	21.75
Damping ratio, ζ	$1.002 \cdot 10^{-1}$	$5.9223 \cdot 10^{-3}$	$1.794 \cdot 10^{-3}$	$4.641 \cdot 10^{-3}$

Table 5-6: Linear approximation non-dimensional coefficients for heave motion.

The damping ratio for all these solutions and their different motions is always in the bracket of zero to one. Therefore, the non-forced oscillations of any of these systems are naturally damped.

The first analysis that we can obtain from the results of tables 5-4 and 5-5 comes from the natural frequencies of oscillation of the different systems. For the surge cases, the natural frequency is very low given the enormous mass of the system. The correspondent natural period in all these cases is in the order of 200 seconds.

This result is definitely noteworthy. We know that the periods of linear oscillations of the platform are in the order of 10 seconds, the same as the periods of the waves that induce these oscillations. Being the natural period of the system so far away from the typical periods of excitation diminishes the necessity for large damping properties of the moor. When the system is forced into an oscillation far away from the natural frequency, the mass and restoring effects do not cancel out. Given that the mass terms of these systems are so large, the inertial effects will absorb the exciting forces regardless of the type of moor present in the system. Therefore, for linear surge oscillations, the damping provided by the moor is not critical towards the design of the platform.

On the other hand, the period of oscillation under slow drift effects is much closer to the natural periods of the platform-moor unit. Thus, a careful study of the damping properties of the system has been done.

Figure 5-3 shows the natural decay of the platform motions given an initial 15 m. offset from the equilibrium position. This figure shows the decay response of the cable and the synthetic solutions for a period of oscillation of 200 seconds.

Given that all the damping ratios are smaller than one, each of these oscillations presents a decaying trend. However, the velocity of decay varies greatly from one solution to another. The rate of decay of the medium and high tension synthetic solutions is far smaller than the other two, and by the time the system has reached 2000 seconds, it continues to oscillate with amplitude equal or higher than 7.5 meters.

Slow drift linear approximation

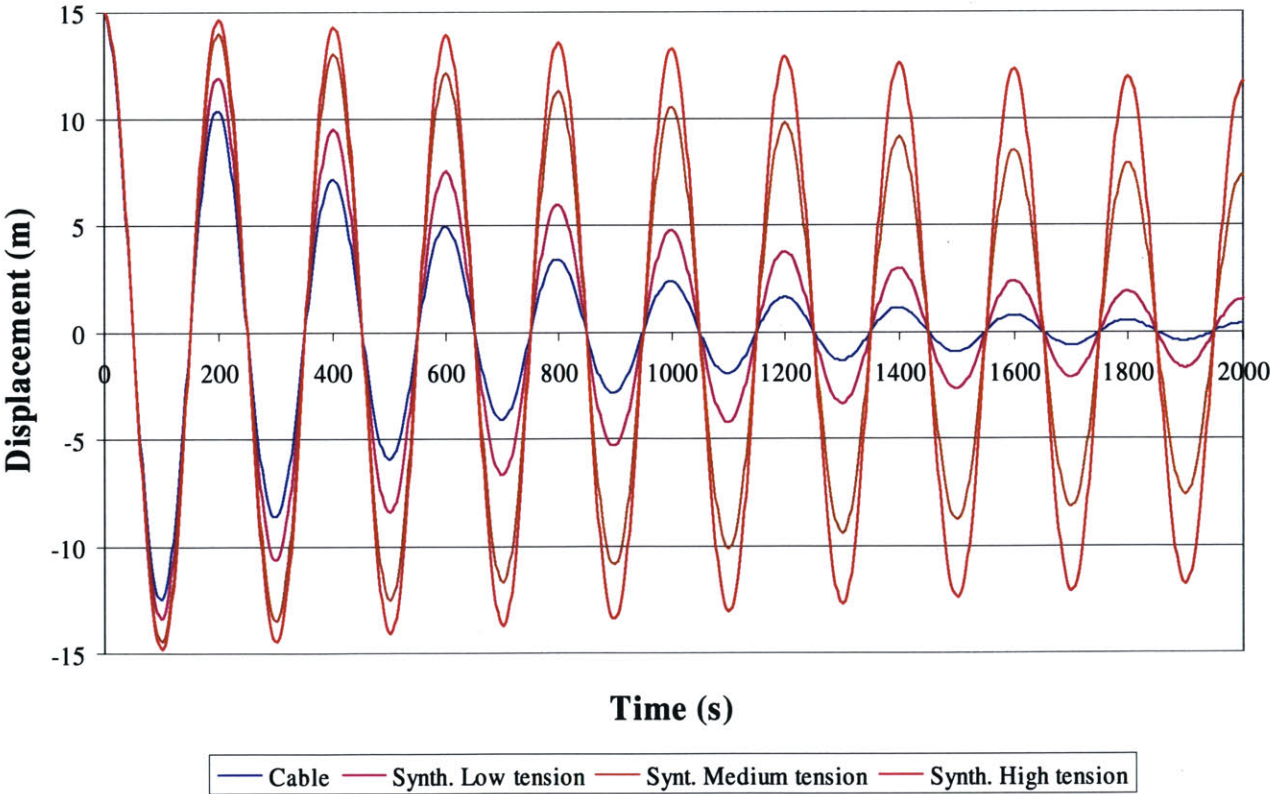


Figure 5-3: Natural oscillation for slow drift linear approximation.

For slow drift motions close to the resonance frequencies of the system, figure 5-3 also shows that the low-tension synthetic moor, even when compared with the cable solution, presents very good damping qualities.

Moreover, the average damping coefficient, used for these approximations, handicaps the results of the low-tension synthetic mooring system. Figures 4-1 and 4-2 show how the damping for the cable decreases as the period of oscillation increases. This pattern is not found in the low-synthetic solution. Therefore, when considering periods as high as 200 seconds, the cable damping is considerably smaller than its average damping. This fact makes the low tension synthetic solution even more attractive, since its respective damping does not decrease with the growth of the period of the oscillations.

Following the same train of thought used for the linear surge, as the slow drift motions move further away from the resonance frequency, the relative importance of the damping in the system diminishes. Therefore, the election of mooring system, when the period of the oscillations are in the order of 1 minute, should not be governed by the damping capabilities of the system. Above all, this study is only considering the damping effects of the mooring system, discharging all the inherit platform viscous damping. If we considered the complete damping, the relative damping difference among the cable and the low-tension synthetic solution will become even smaller.

Regarding the oscillations in heave, we can see in table 5-6, that the natural period of these systems are in general very large compared to the period of the exciting waves. This is clearly the case for all solutions apart from the high-tension synthetic moor. An analogy to the linear surge case can then be established. In general, the motions in heave will be most affected by the mass of the platform. This factor along with the exciting force will determine the nature of the motions regardless of the mooring system used. Note that for a SPAR platform in this mode, motions in this mode of oscillation, will be typically very small, given the very large depth of the body and its vertical cylindrical shape. The only surface on the floating body where pressure can cause vertical resulting

forces is on its' bottom, and at a depth of 200 meters, the wave effects create very small variations in the overall pressure of the fluid.

Unless the mooring system is very taut, and thus its natural period becomes close to the period of the exciting waves, the damping contributions of the moor in vertical direction are not a major concern for the dynamics of the platform.

CHAPTER 6:

CONCLUSIONS

As the water depth for offshore oil drilling increases, the trend in the mooring systems design is shifting from classical cable mooring line into solutions based of synthetic ropes.

The mechanical responses, especially to dynamic excitations, of these synthetic moor solutions, under very large water depth conditions, have not yet been tested.

There are several reasons for the consideration of light synthetic rope solutions, among which, the most significant is based purely on economics. Not only the cheaper cost of the synthetics, but also, its lower cost of installation make them an extremely attractive alternative for large and very large water depths.

Regarding the mechanical properties of the synthetic mooring systems, Chapter 3 demonstrates that the restoring forces achieved by regular catenary-type moor can be easily attained by light taut mooring systems.

These restoring forces, however, can create misleading interpretations. The fact that the moor is more taut does not automatically imply smaller oscillations of the moored floating body. In the case of the mooring systems considered in this thesis, the mass of the platform is so vast that the inertial terms of the motion equation govern the response of the system to external loads. Therefore, the amplitude of the motions when the offshore platform is forced to oscillate under external loads will not vary significantly from one mooring system to another. The damping becomes a second-order consideration.

If one further increased the initial pretension of the synthetics, provided that the maximum tension in the lines was not a critical concern, this increase would only make the natural frequency of the heave response to move towards the frequency of the waves that generates that heave. Then, the amplitude of the oscillations would become dangerous for the integrity of the moor.

Regarding the dynamic responses, and particularly the damping that the system introduces into the platform motions, Chapter 5 shows that only the damping qualities of the moor regarding slow-drift oscillations are critical when designing spread-mooring systems for large water depths.

In Chapter 5 we also proved that the low-tension synthetic mooring solution presents excellent dynamic properties. It provides the platform with restoring forces even larger than the original cable solution as well as behaves favorably under slow-drift oscillations. A fully coupled platform-mooring system numerical analysis would provide a more accurate solution and could be utilized to ensure the validity of these results.

These considerations about the low-tension synthetic moor, added to its lower cost, make this a viable alternative for the positioning and control of floating structures in large water depths.

REFERENCES:

- [1] Cannon, Dynamics of physical systems
- [2] Michael S. Triantafyllou, Mooring Dynamics for offshore applications. Part one I. Theory.
- [3] Genevieve Tcheou, Non-Linear dynamics of mooring lines
- [4] Finn Gunnar Nielsen, Arne Ulrik Bindingsb*, Extreme loads in taut mooring lines and mooring line induced damping. An asymptotic approach.
- [5] F.G. Nielsen, A.U. Bindingsb*, Alternative configurations and materials for deep water mooring. Results from a three year joint research effort. OTC Paper 10755.
- [6] John Magne Johnsen , Ola Øritsland, Design and optimisation of Taut-leg mooring systems. OTC Paper 10776.
- [7] Ivan De Pellegrin, Manmade fiber ropes in deepwater mooring applications. OTC Paper 10907.
- [8] D. L. Garret, Dynamic analysis of slender rods
- [9] William C. Webster, Mooring-induced damping
- [10] Boston Marine Consulting Inc. LINES 1.1 User Manual
- [11] R. M. Raaijmakers and J.A. Battjes, An experimental verification of Huse's model on the calculation of mooring line damping.
- [12] A.C. Fernandes, M. M. Mourelle, O.B. Sert♦, S. da Silva and P.H.C.C. Parra, Hydrodynamic coefficients in the design of steel catenary risers.

[13] C.R. Chaplin, Reading U. and C.J.M. Del Vecchio, Appraisal of lightweight moorings for deep water. OTC 6965.

[14] Bob Wilde, Patrick Kelly, Filippo Librino, and Simeon Whitehill, Conceptual design and comparison of aramid and polyester taut leg spread moorings for deep water applications. OTC Paper 8145.

APPENDIX A: ROPE PROPERTIES

Polyester rope properties:

Breaking Strength (N)	Weigh in air (N/m)	Weigh in water (N/m)	Diameter (m)	EA (N)
6.23E+06	159.3856	40.97654	0.154178	95898880
6.67E+06	171.6348	44.18467	0.16002	1.03E+08
7.12E+06	184.0299	47.24698	0.165608	1.1E+08
7.56E+06	196.4249	50.4551	0.171196	1.16E+08
8.01E+06	208.82	53.66323	0.17653	1.23E+08
8.45E+06	221.3608	56.87136	0.18161	1.3E+08
8.90E+06	234.0475	60.07949	0.18669	1.37E+08
9.34E+06	202.8412	63.43344	0.19177	1.44E+08
9.79E+06	257.8168	66.64157	0.196596	1.51E+08
1.02E+07	271.9618	69.8497	0.201422	1.58E+08
1.07E+07	284.7943	73.20365	0.205994	1.64E+08
1.11E+07	297.481	76.41178	0.210566	1.71E+08
1.16E+07	310.4593	79.76573	0.215138	1.78E+08
1.20E+07	323.2918	83.11968	0.219456	1.85E+08
1.25E+07	336.1243	86.32781	0.223774	1.92E+08
1.29E+07	349.1027	89.68176	0.228092	1.99E+08
1.33E+07	362.081	93.03571	0.23241	2.05E+08

Aramid rope properties:

Breaking Strength (N)	Weigh in air (N/m)	Weigh in water (N/m)	Diameter (m)	EA Soft (N)	EA Stiff (N)
6.67E+06	77.1409	21.58195	0.09906	1.11E+08	2.22E+08
7.12E+06	82.39056	23.04019	0.104902	1.18E+08	2.36E+08
7.56E+06	87.4944	24.49843	0.108966	1.25E+08	2.51E+08
8.01E+06	92.59824	25.95667	0.112014	1.32E+08	2.65E+08
8.45E+06	97.8479	27.41491	0.115062	1.4E+08	2.79E+08
8.90E+06	102.9517	28.87315	0.119126	1.47E+08	2.94E+08
9.34E+06	108.0556	30.33139	0.122174	1.09E+08	3.08E+08
9.79E+06	113.1594	31.64381	0.125222	1.61E+08	3.22E+08
1.02E+07	118.4091	33.10205	0.12827	1.68E+08	3.36E+08
1.07E+07	123.5129	34.56029	0.131318	1.76E+08	3.51E+08
1.11E+07	128.6168	36.01853	0.13462	1.83E+08	3.65E+08
1.16E+07	134.0123	37.47677	0.137668	1.9E+08	3.79E+08
1.20E+07	138.9703	38.93501	0.140716	1.97E+08	3.94E+08
1.25E+07	144.0741	40.39325	0.143764	2.04E+08	4.08E+08
1.29E+07	149.3238	41.85149	0.146812	2.12E+08	4.22E+08
1.33E+07	154.4276	43.1639	0.150114	2.19E+08	4.37E+08